2020
NOVEMBER
19
Thursday

seminar

WE HAVE A NEW LIQUID CRYSTAL THAT FORMS HELICAL STRUCTURES ... AND WHAT NEXT ?

Anna DRZEWICZ

Department of Soft Matter Research
Division of Condensed Matter Physics
The Henryk Niewodniczański Institute of Nuclear Physics Polish Academy of Sciences

https://orcid.org/0000-0002-1483-5645

anna.drzewicz@ifj.edu.pl

What are liquid crystals?

crystal

isotropic liquid

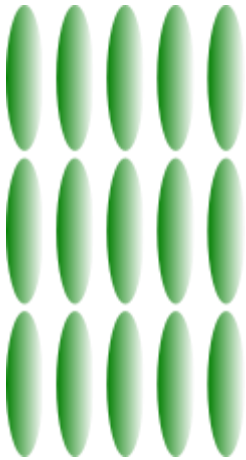

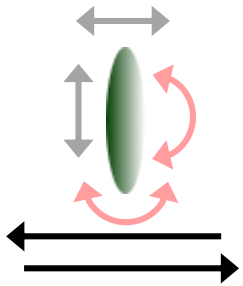

F. Reinitzer

O. Lehmann

increase of temperature

What are liquid crystals?

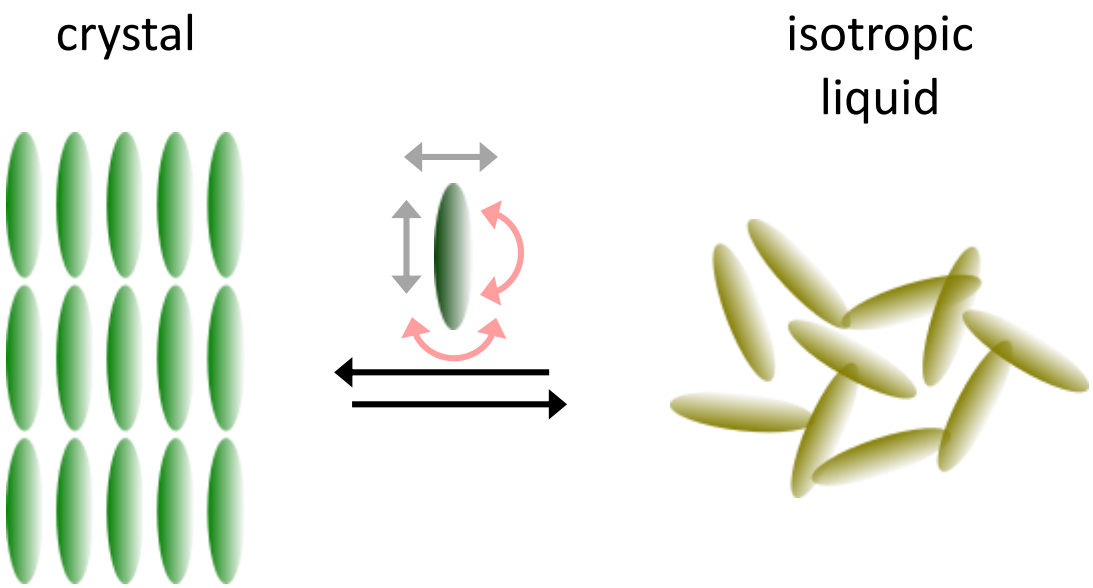

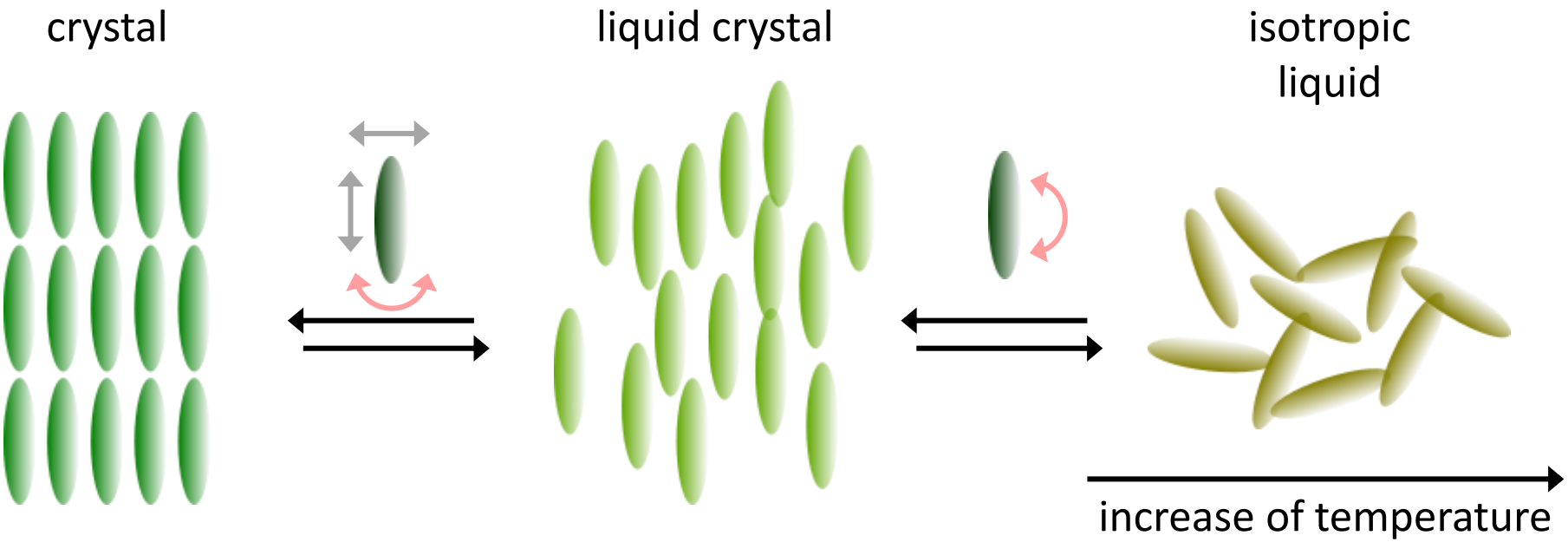

Today we know tens of thousands of liquid crystal compounds

thermotropic

lyotropic

spherical

oblong

flat

cubicoid

bent

bowl-shaped

nematic

smectic

cubic

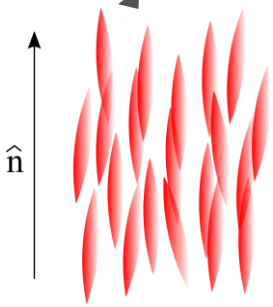

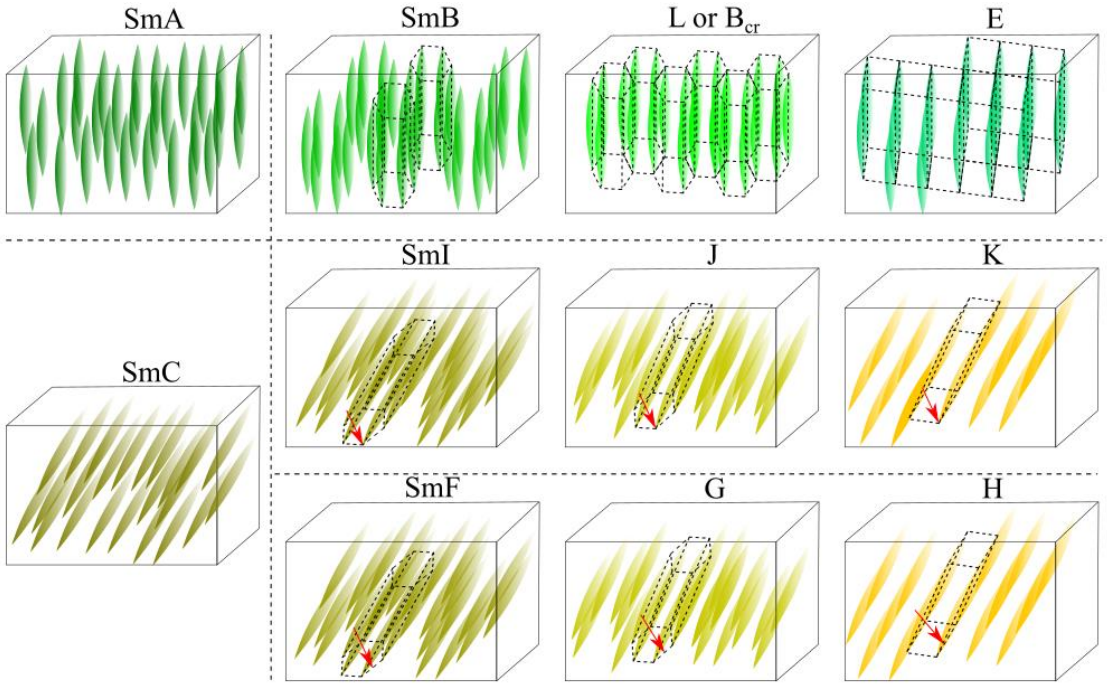

Chiral smectic phases

SmC phase

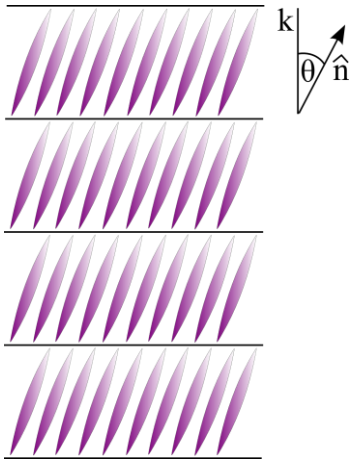

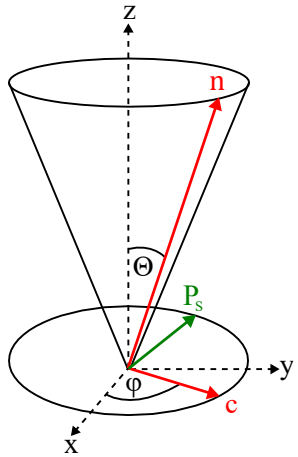

SmC* phase

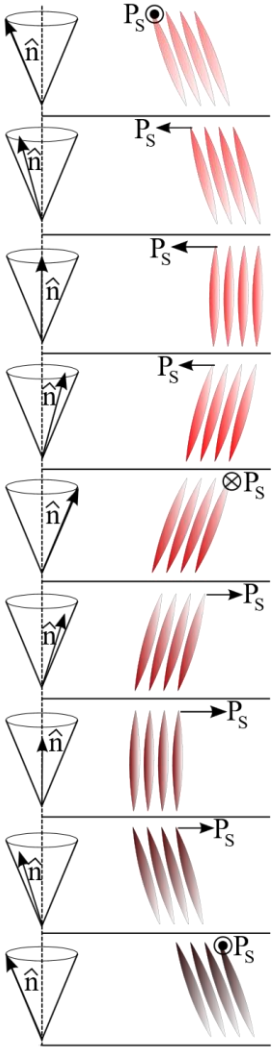

SmC_A phase

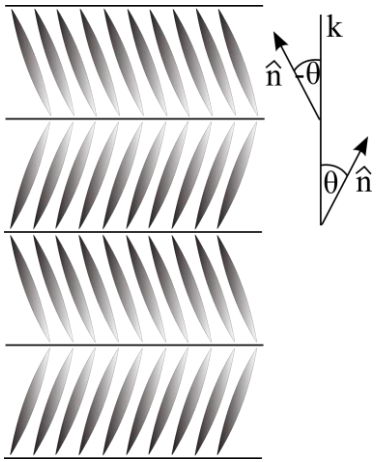

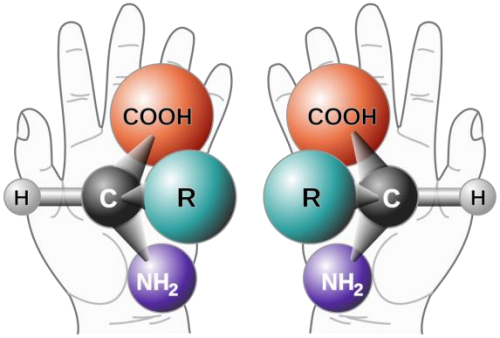

SmC_A* phase

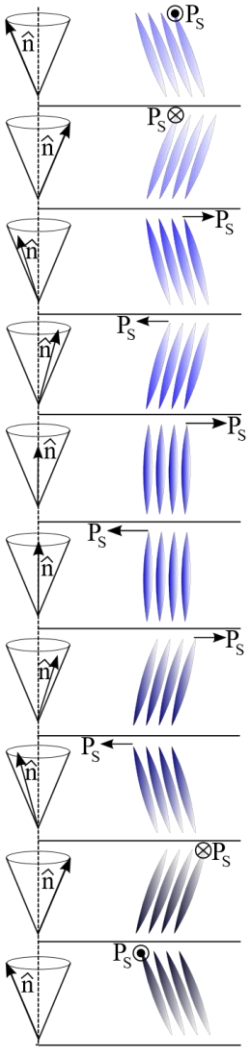

Material

3F7HPhH7

(S)- 4’-(1-methyloctyloxycarbonyl)biphenyl-4-yl 4-[7-(2,2,3,3,4,4,4-heptafluorobutoxy)-heptyl1-oxy]-benzoate

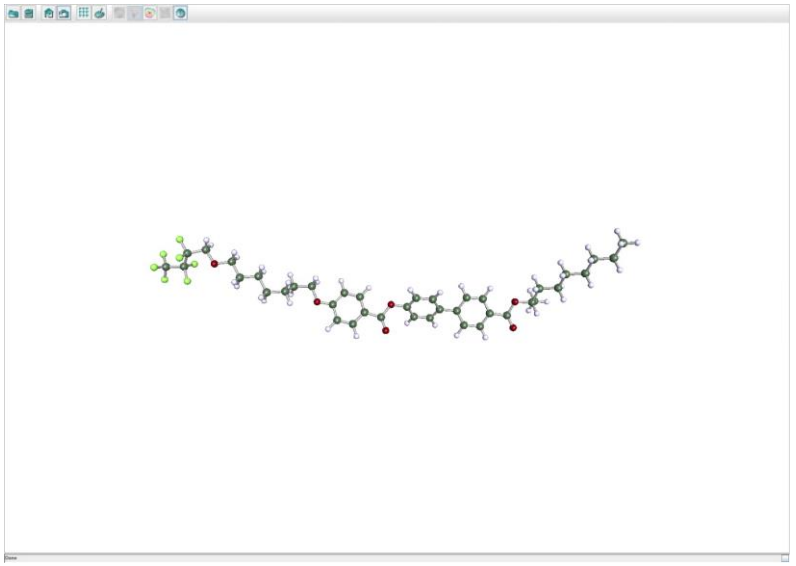

perfluorinated chain

C=O groups

chiral centre

-C
-F
-H
-O

Molecule optimized by DFT method (def2-TZVPPD basis and B3–LYP).
Dipole moment components, determined by AIM method, are: $\mu_x = 0.073, \mu_y = 0.43, \mu_z = -2.30$.
Dipole moment μ equals 5.9 D (OZ axis is perpendicular to the long molecular axis).

M. Żurowska, R. Dąbrowski, J. Dziaduszek, K. Garbat, M. Filipowicz, M. Tykarska, W. Rejmer, K. Czupryński, A. Spadło, N. Bennis, JM. Otón, *J. Mater. Chem.*, **2011**, 21, 2144
K. Milewska, W. Drzewiński, M. Czerwiński, R. Dąbrowski, *Liq. Cryst.*, **2015**, 42(11), 1601

Why this compound?

Fluorinated compounds are very good stabilizers for liquid crystal mixtures for applications.

It undergoes vitrification and cold crystallization processes.

The presence of carbonyl groups has an influence on the dielectric anisotropy, a key feature making a particular liquid crystal material suitable for use in display devices.

The long conjugated electronic system of π–bonds causes a high value of birefringence of molecules.

The presence of chiral centre favours the formation of a helical structure in some liquid crystal phases and such substances can be used e.g. in human body temperature sensors.

Why this compound?

Fluorinated compounds are very good stabilizers for liquid crystal mixtures for applications.

It undergoes vitrification and cold crystallization processes.

The presence of carbonyl groups has an influence on the dielectric anisotropy, a key feature making a particular liquid crystal material suitable for use in display devices.

Glass of liquid crystals:

- ✓ electro-optical devices for selective reflection of light;
- ✓ manufacturing amorphous pharmaceuticals or drug carriers, assuring a better bioavailability of active substances.

The long conjugated electronic system of π–bonds causes a high value of birefringence of molecules.

The presence of chiral centre favours the formation of a helical structure in some liquid crystal phases and such substances can be used e.g. in human body temperature sensors.

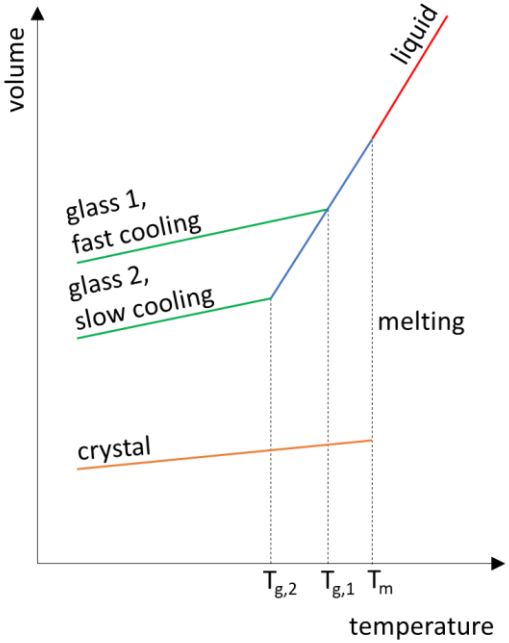

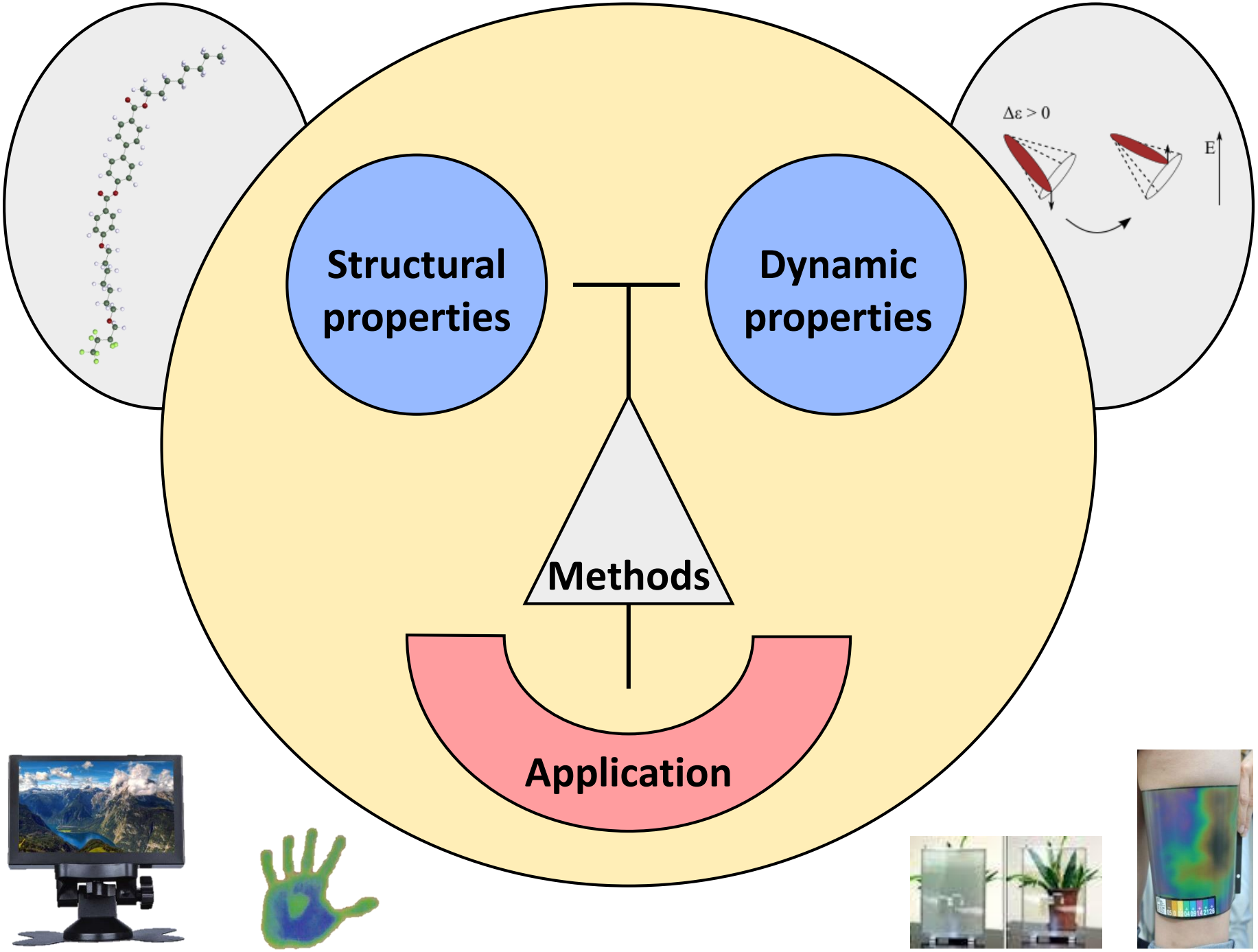
Structural properties
Dynamic properties
Methods
Application
Δε > 0
E

Methods

Differential Scanning Calorimetry (DSC)

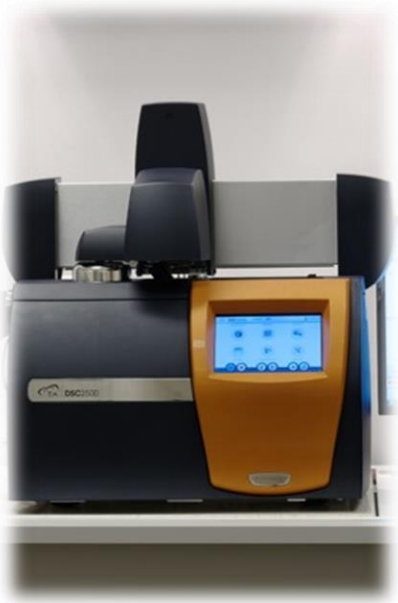

Polarized Optical Microsopy (POM)

Thermooptic Analysis (TOA)

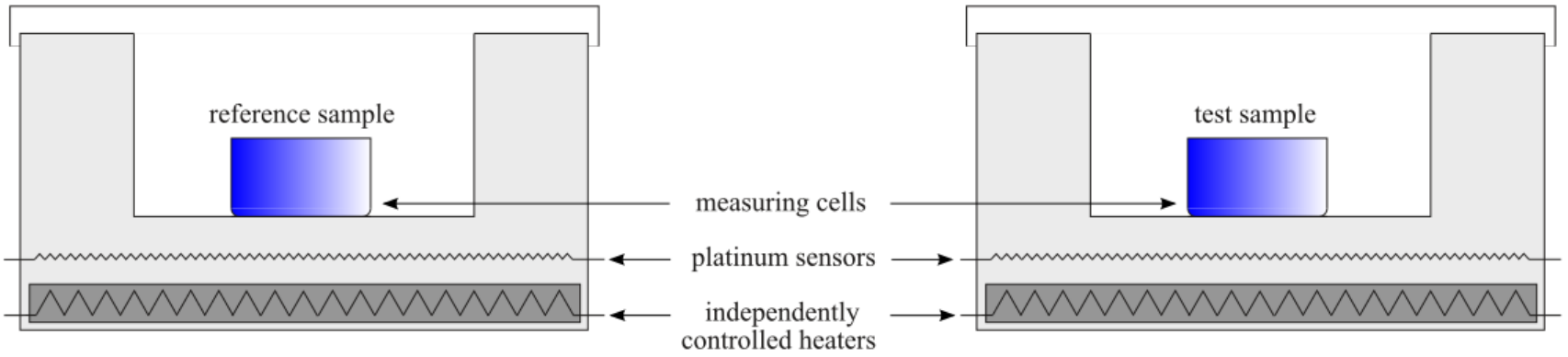

https://www.ifj.edu.pl/oddzialy/no3/nz35/

Methods

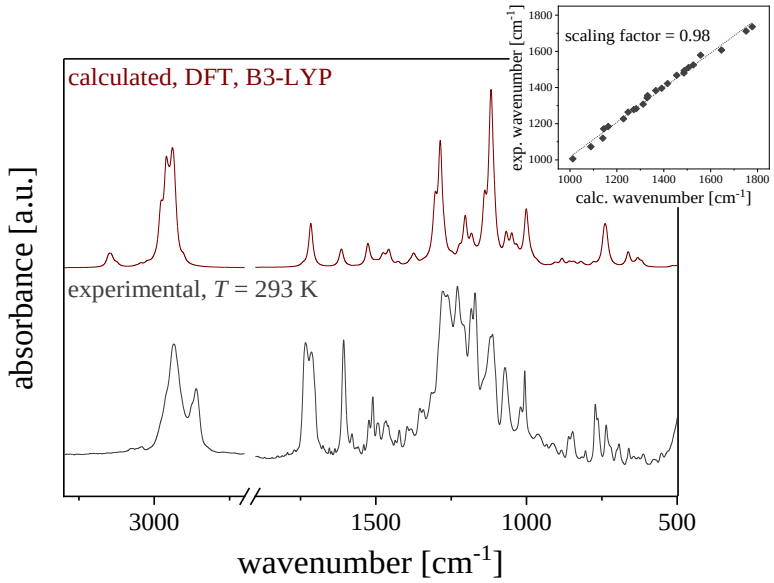

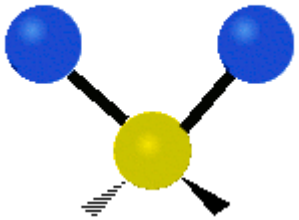

symmetric stretching

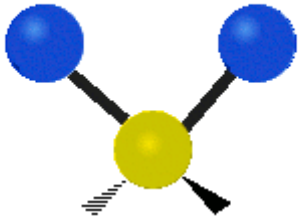

asymmetric stretching

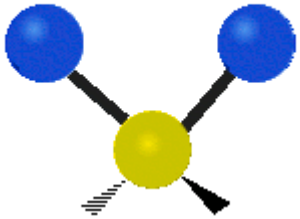

scissoring

Fourier Transform Infrared Spectroscopy (FTIR)

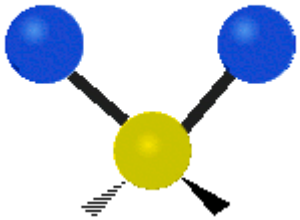

rocking

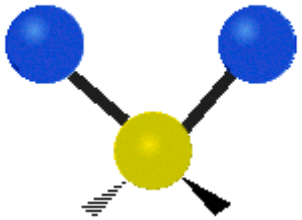

wagging

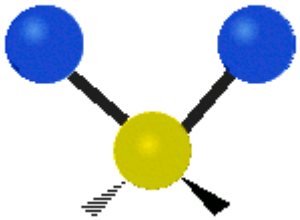

twisting

https://www.ifj.edu.pl/oddzialy/no3/nz35/

Methods

Differential Scanning Calorimetry (DSC)

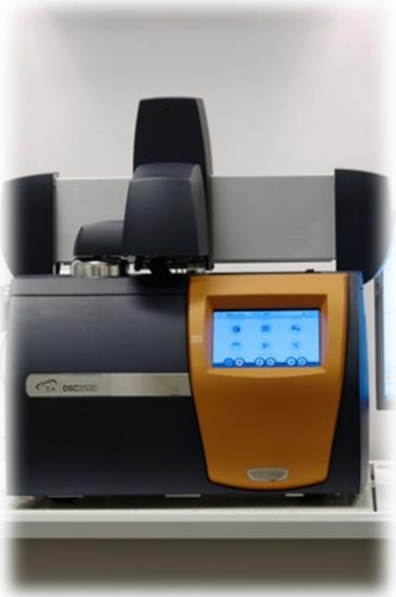

Polarized Optical Microsopy (POM)

Thermooptic Analysis (TOA)

Fourier Transform Infrared Spectroscopy (FTIR)

Broadband Dielectric Spectroscopy (BDS)

https://www.ifj.edu.pl/oddzialy/no3/nz35/

What is the Phase Behaviour?

Phase behaviour of 3F7HPhH7

DSC recorded for a cooling/heating rate of 8 K/min

cooling

phase transition	$T_{p.t.}$ [K]	$\Delta H_{p.t.}$ [kJ/mol]	$\Delta S_{p.t.}$ [Jmol^{-1}K^{-1}]
Iso – SmA	389.5	1.9	4.9
SmA – SmC*	388.1	0.7	1.8
SmC* – SmC$_A^*$	374.7	0.02	0.1
SmC$_A^*$ – gSmC$_A^*$	257.8	-	-

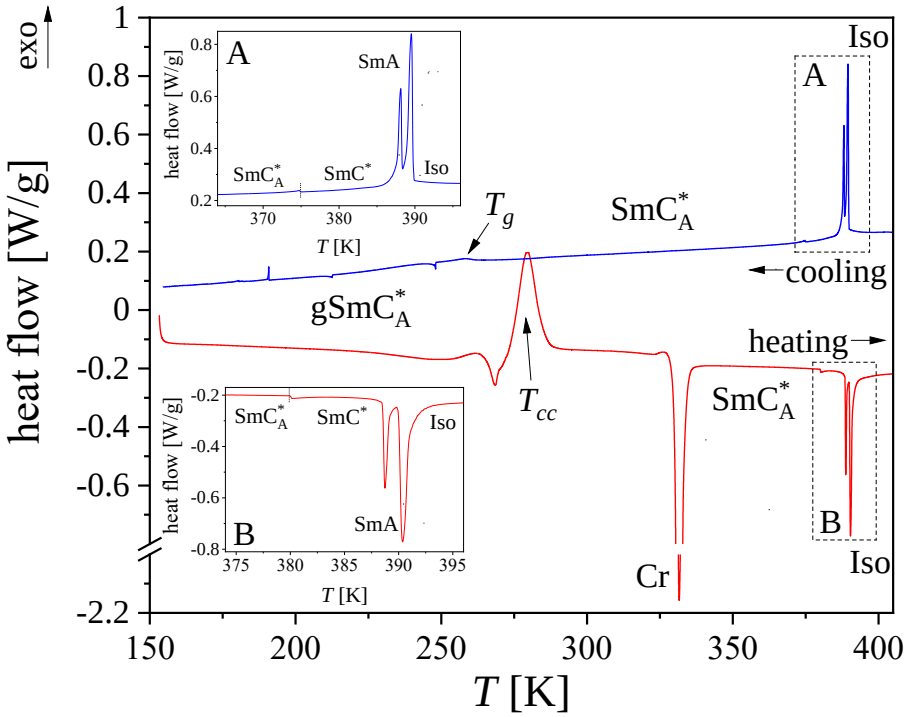

heating

phase transition	$T_{p.t.}$ [K]	$\Delta H_{p.t.}$ [kJ/mol]	$\Delta S_{p.t.}$ [Jmol^{-1}K^{-1}]
gSmC$_A^*$ – Cr	279.4	15.2	54.5
Cr – SmC$_A^*$	331.6	27.3	82.5
SmC$_A^*$ – SmC*	380.2	0.1	0.2
SmC* – SmA	388.7	0.7	1.8
SmA – Iso	390.4	2.5	6.5

DSC (cooling)

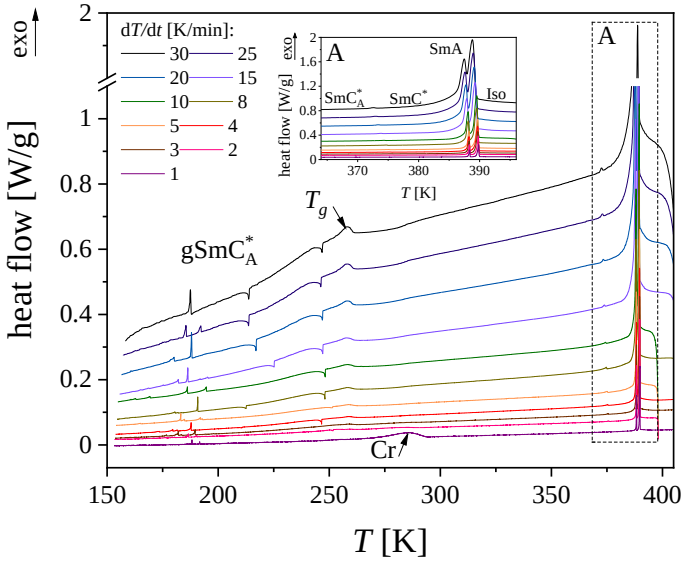

DSC (heating)

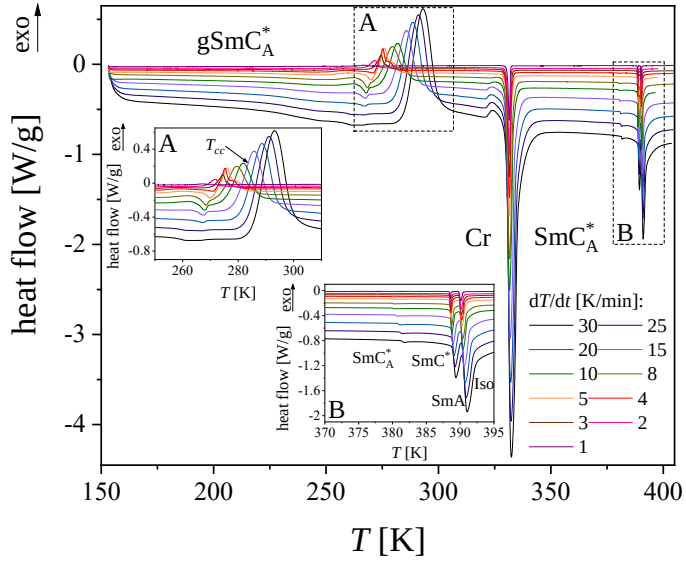

A. Drzewicz, E. Juszyńska-Gałązka, W. Zając, M. Piwowarczyk, W. Drzewiński, *J. Mol. Liq.*, **2020**, 319, 114153

Phase behaviour of 3F7HPhH7

POM textures observed during

cooling

heating

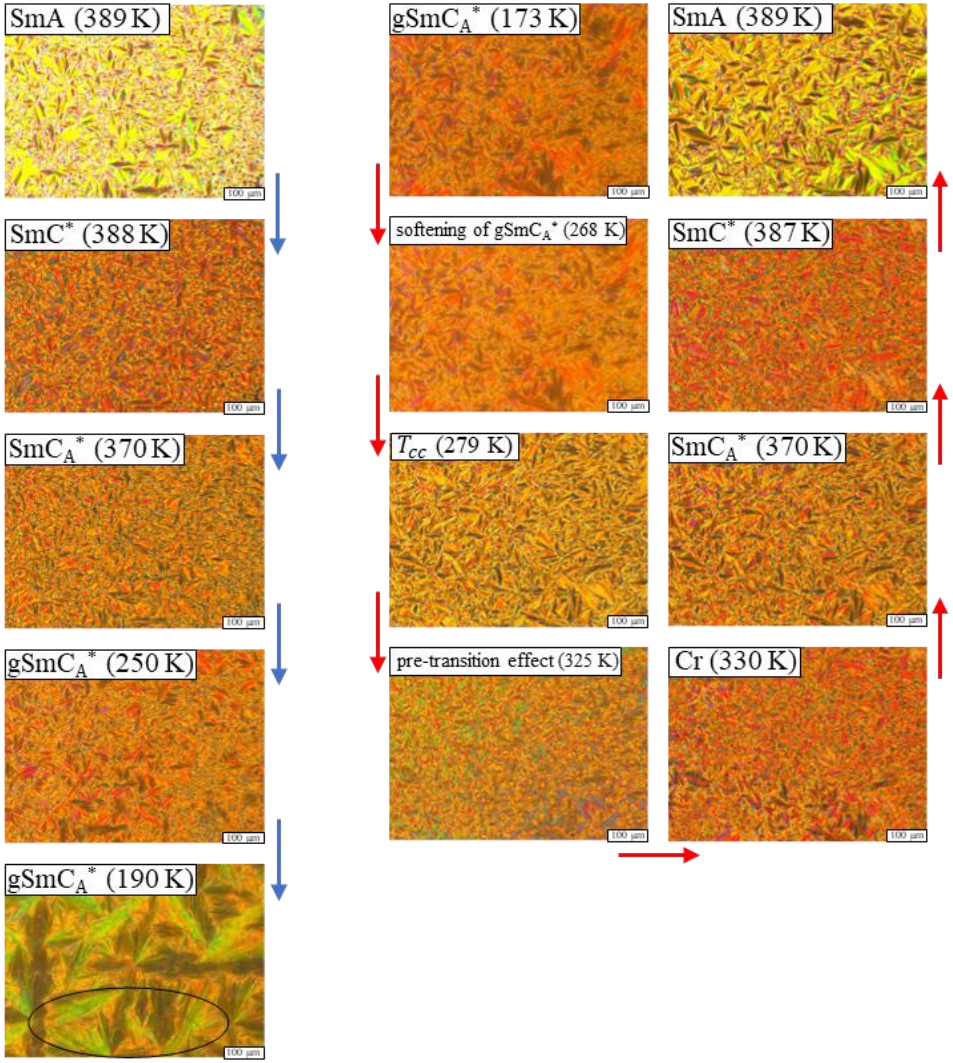

TOA and DSC (cooling)

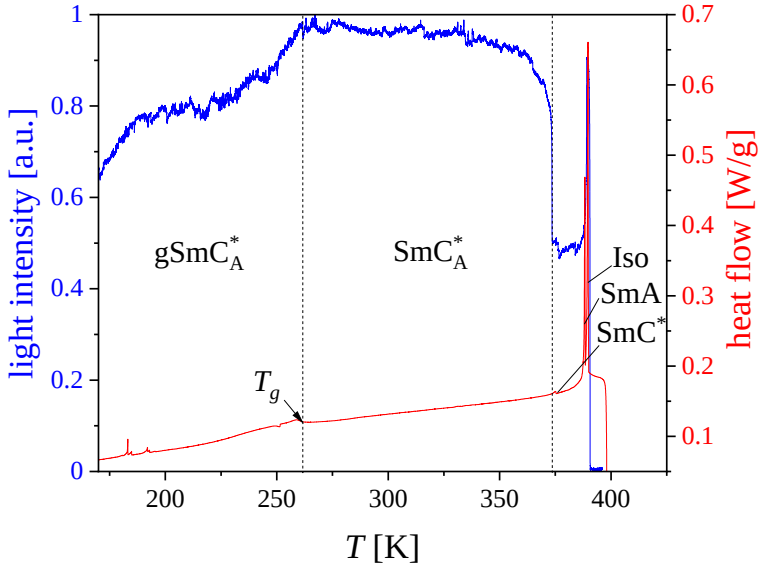

TOA and DSC (heating)

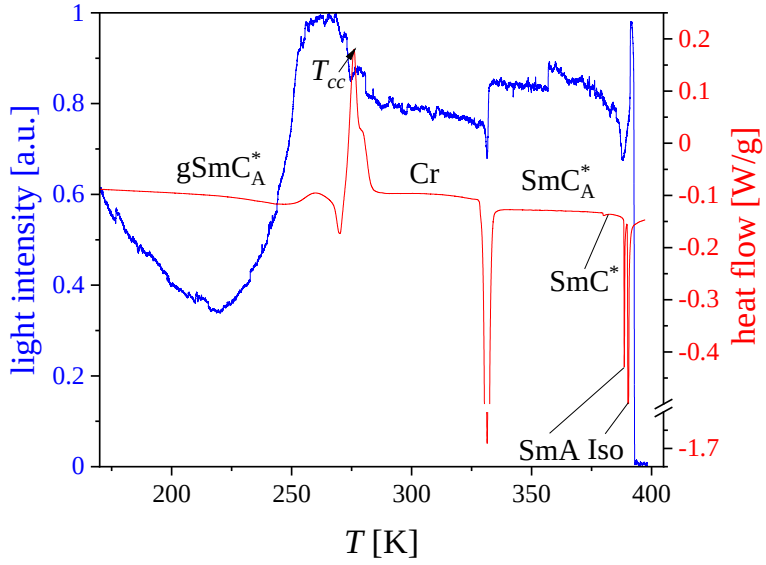

A. Drzewicz, E. Juszyńska-Gałązka, W. Zając, M. Piwowarczyk, W. Drzewiński, *J. Mol. Liq.*, **2020**, 319, 114153

What happens during Slow Cooling and next Heating?

Slow cooling and next heating of 3F7HPhH7

DSC thermograms

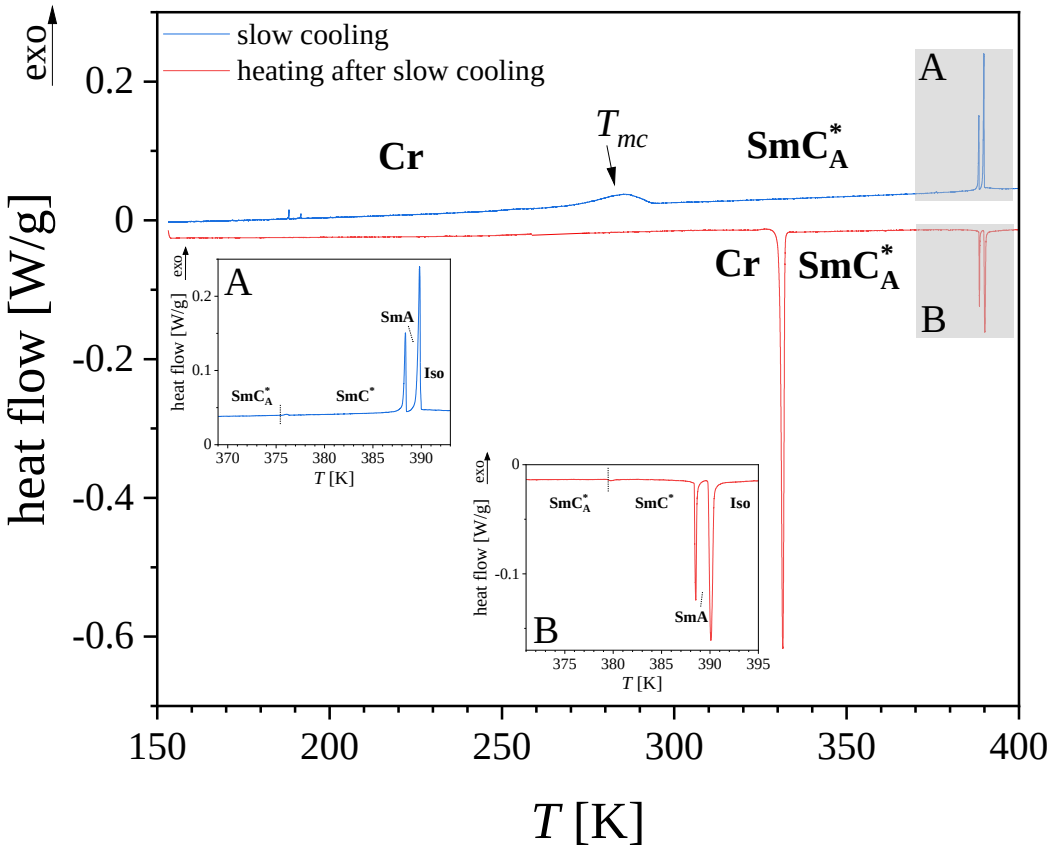

DSC and **BDS** (cooling)

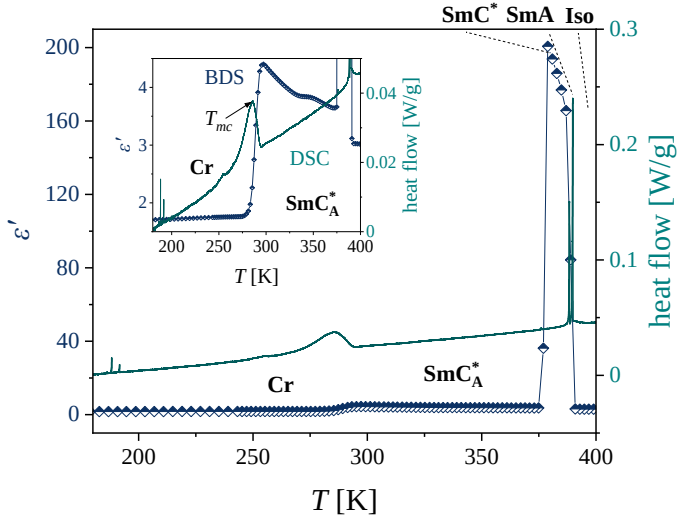

DSC and **BDS** (heating)

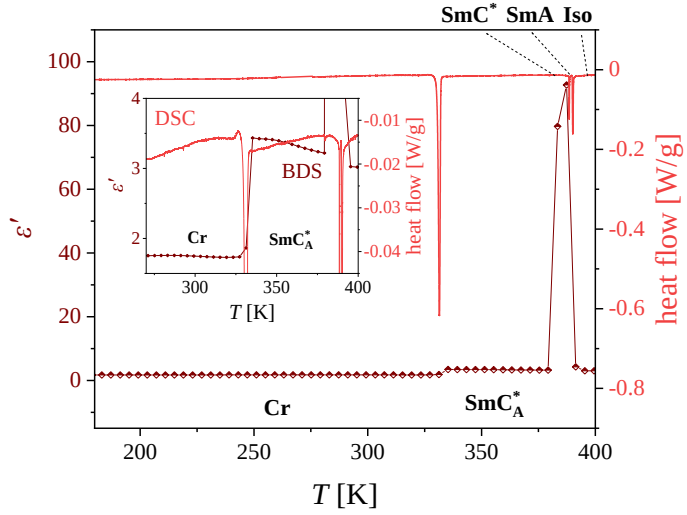

A. Drzewicz, M. Jasiurkowska-Delaporte, E. Juszyńska-Gałązka, M. Piwowarczyk, W. Zając, P. Kula, *On relaxation dynamics of double glass-forming antiferroelectric liquid crystal*, prepared

Idea of BDS

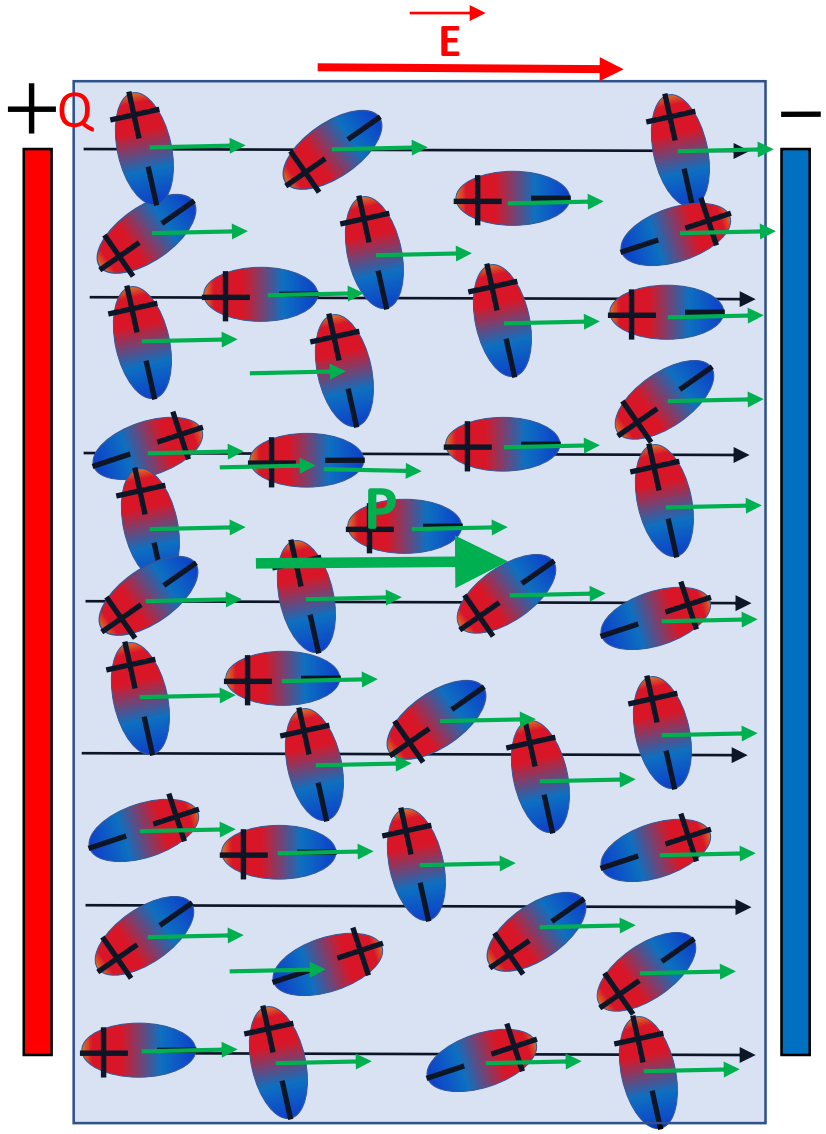

The scheme of parallel-plate capacitor with a dielectric material

Relaxation dynamics of 3F7HPhH7 during slow cooling

Dielectric loss ε'' vs. frequency ν observed during slow cooling (**BDS**)

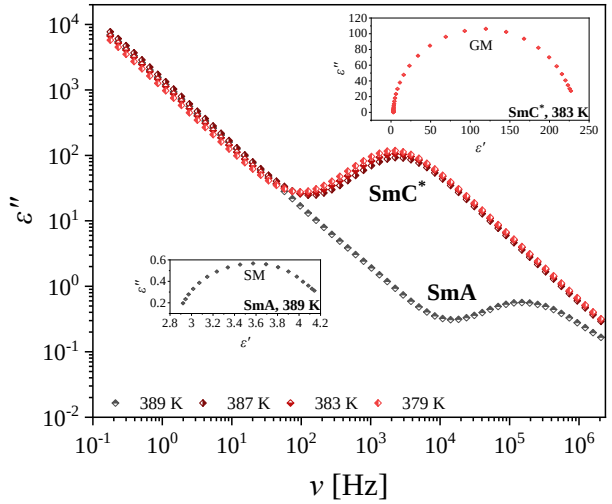

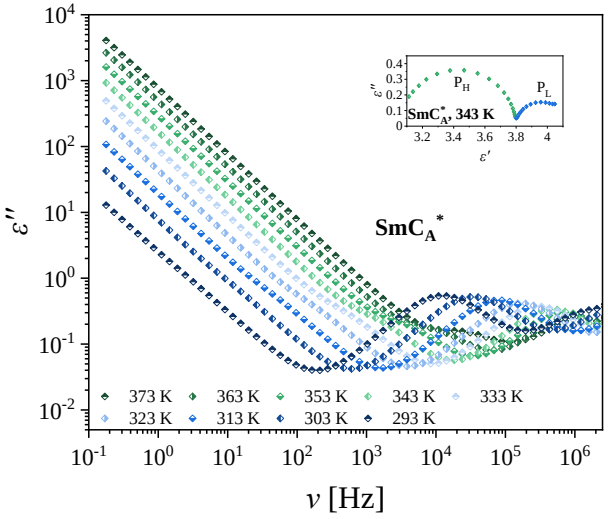

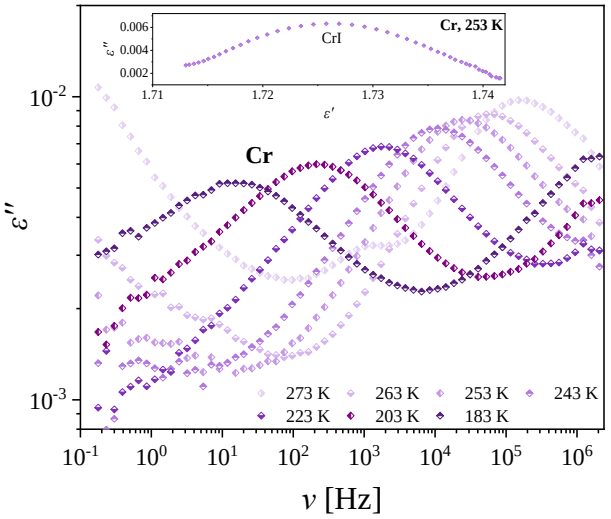

Dielectric loss ε'' vs. frequency ν observed with the bias field applied (**BDS**)

amplitudon

phasons

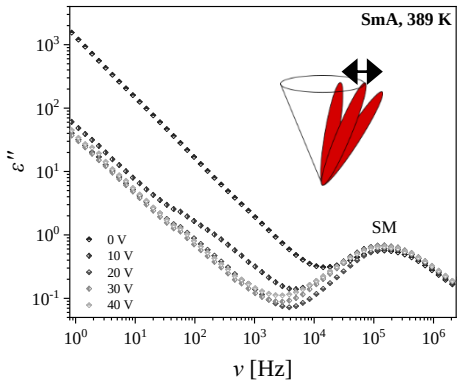

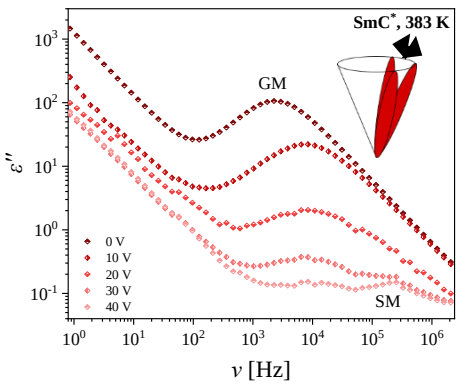

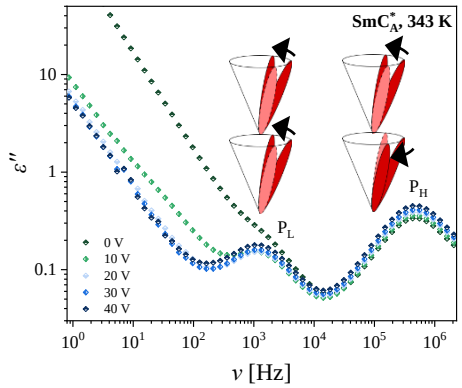

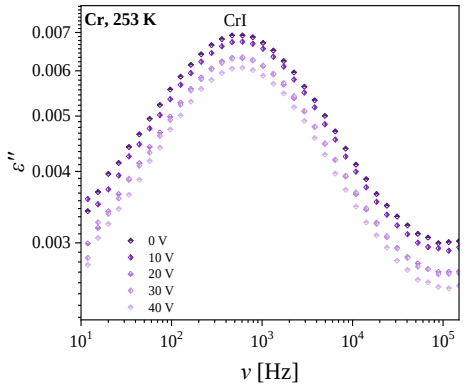

A. Drzewicz, M. Jasiurkowska-Delaporte, E. Juszyńska-Gałązka, M. Piwowarczyk, W. Zając, P. Kula, *On relaxation dynamics of double glass-forming antiferroelectric liquid crystal*, prepared

Relaxation dynamics of 3F7HPhH7 during slow cooling and heating

Activation plots during slow cooling (full points) and heating (open points)

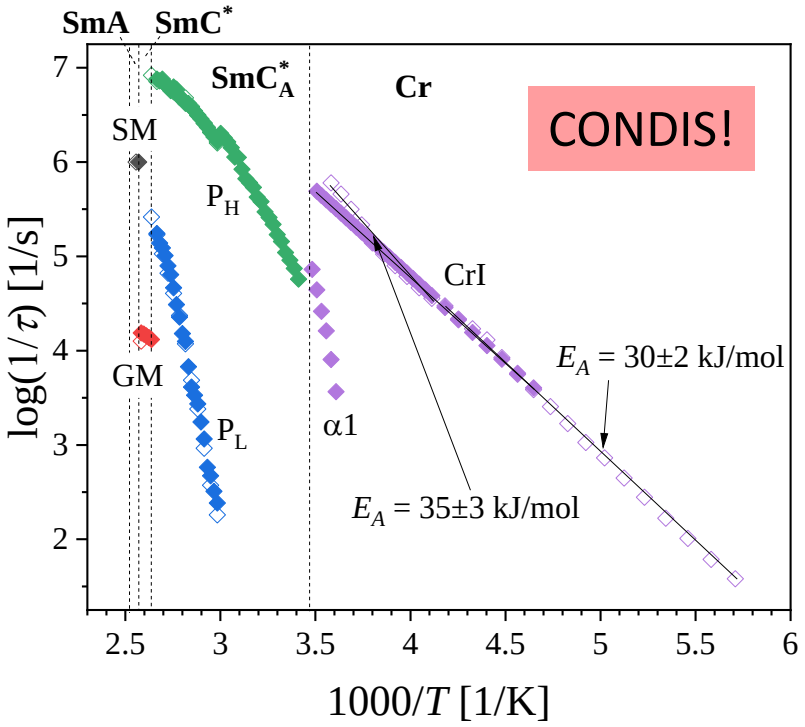

$$\Delta S_{Cr\rightarrow SmC_A^*} = 34 \pm 1\ \mathrm{Jmol^{-1}K^{-1}}$$

Arrhenius equation:

$$\ln k = -\frac{E_A}{RT} + \ln A$$

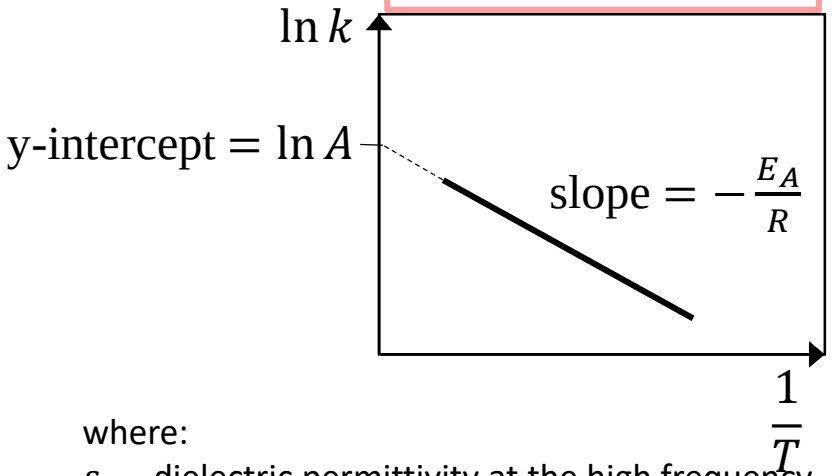

Havriliak-Negami equation (HN):

$$\varepsilon^*(\omega) = \varepsilon_\infty + \sum_k \frac{\Delta\varepsilon_k}{\left[1 + \left(i\omega\tau_{HN_k}\right)^{\alpha_{HN_k}}\right]^{\beta_{HN_k}}} + \frac{\sigma_0}{\omega\varepsilon_0}$$

where:
ε_∞ - dielectric permittivity at the high frequency,
$\Delta\varepsilon_k$ - dielectric strength of k-process,
τ_{HN_k} - relaxation time of k-process,
σ_0 - dc electrical conductivity,
ε_0 - dielectric permittivity of the vacuum,
$\alpha_{HN_k}, \beta_{HN_k}$ - shape parameters describe symmetric and asymmetric broadening of loss spectra.

A. Drzewicz, M. Jasiurkowska-Delaporte, E. Juszyńska-Gałązka, M. Piwowarczyk, W. Zając, P. Kula, *On relaxation dynamics of double glass-forming antiferroelectric liquid crystal*, prepared
S. Havriliak, S. Negami, *Polymer (Guildf)*, **1967**, 8, 161; F. Alvarez, A. Alegría, J. Colmenero, *Phys. Rev. B.*, **1993**, 47, 125

Relaxation dynamics of 3F7HPhH7 during slow cooling and heating

Activation plots during slow cooling (full points) and heating (open points)

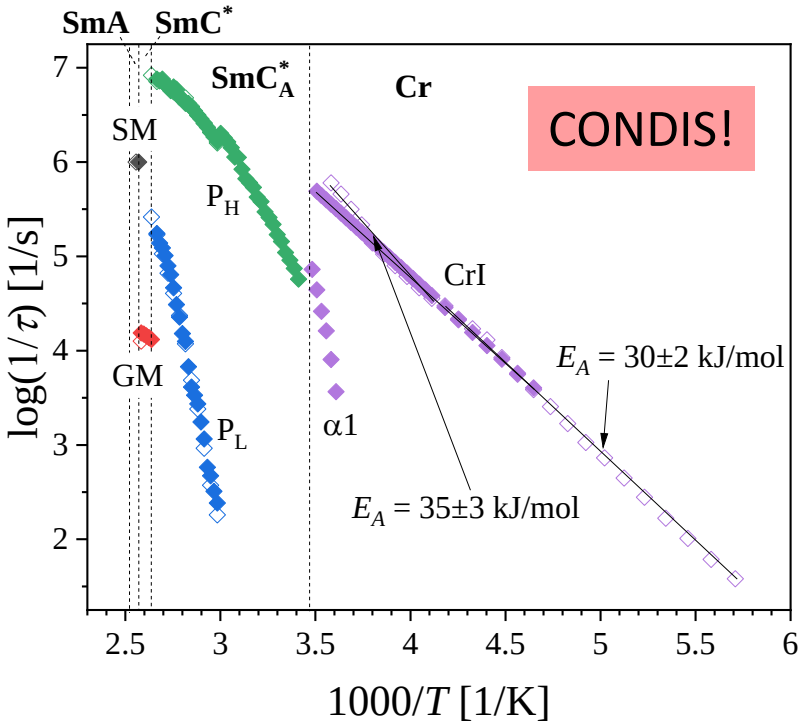

$$\Delta S_{Cr\rightarrow SmC_A^*} = 34 \pm 1\ \mathrm{Jmol^{-1}K^{-1}}$$

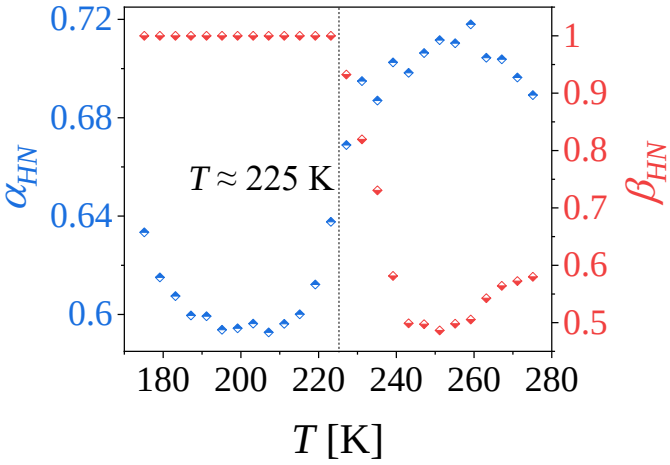

Havriliak-Negami equation (HN):

$$\varepsilon^*(\omega) = \varepsilon_\infty + \sum_k \frac{\Delta\varepsilon_k}{\left[1 + \left(i\omega\tau_{HN_k}\right)^{\alpha_{HN_k}}\right]^{\beta_{HN_k}}} + \frac{\sigma_0}{\omega\varepsilon_0}$$

where:
ε_∞ - dielectric permittivity at the high frequency,
$\Delta\varepsilon_k$ - dielectric strength of k-process,
τ_{HN_k} - relaxation time of k-process,
σ_0 - dc electrical conductivity,
ε_0 - dielectric permittivity of the vacuum,
$\alpha_{HN_k}, \beta_{HN_k}$ - shape parameters describe symmetric and asymmetric broadening of loss spectra.

A. Drzewicz, M. Jasiurkowska-Delaporte, E. Juszyńska-Gałązka, M. Piwowarczyk, W. Zając, P. Kula, *On relaxation dynamics of double glass-forming antiferroelectric liquid crystal*, prepared
S. Havriliak, S. Negami, *Polymer (Guildf)*, **1967**, 8, 161; F. Alvarez, A. Alegría, J. Colmenero, *Phys. Rev. B.*, **1993**, 47, 125

What happens upon Pressure?

BDS measurements upon pressure

Range of pressure: up to **600 Mpa**
Range of temperature: **253 K – 393 K**
Average temperature increment upon heating and cooling: **2 K/min**
Pressure medium: nonpolar **silicon oil**

p is approx. 6 times greater than p in the deepest point of the Marian Trench (110 MPa there)!!!

https://www.scientificamerican.com/article/the-mariana-trench-is-7-miles-deep-whats-down-there/

Relaxation dynamics in SmC_A^* phase at ambient and elevated pressure

Dielectric loss ε'' vs. frequency ν measured at one isotherm at 333 K (**BDS**)

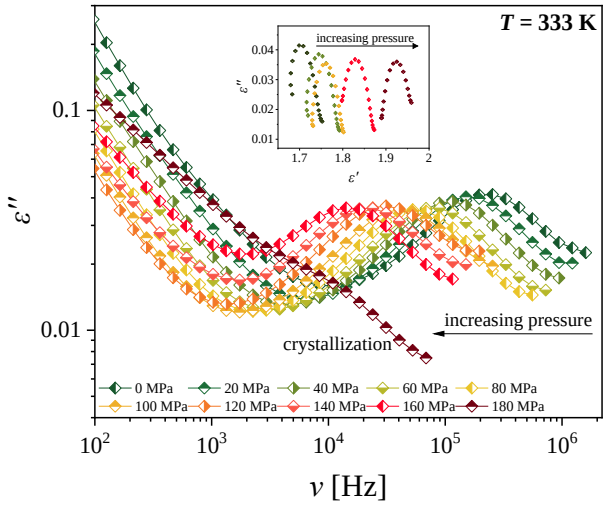

Activation volume

$$\Delta^{\#}V$$

$$\Delta^{\#}V = RT(\partial \ln \tau / \partial p)_T$$

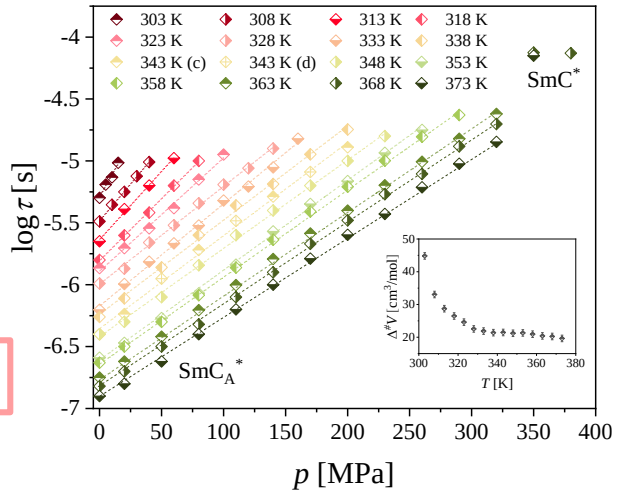

Dielectric loss ε'' vs. frequency ν measured at one isobar at 110 MPa (**BDS**)

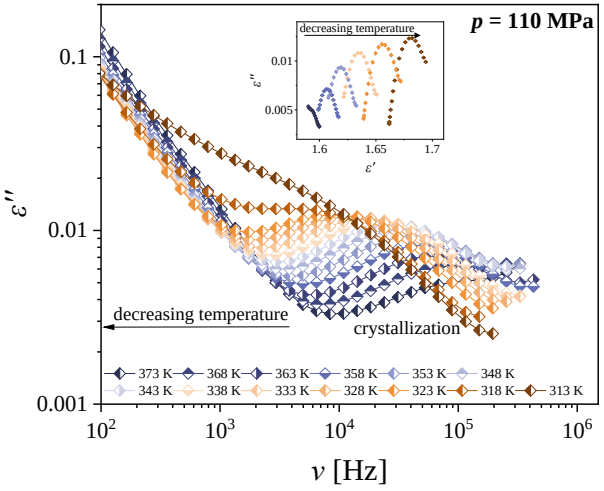

Activation enthalpy $\Delta^{\#}H$:

$$\Delta^{\#}H = RT(\partial \ln \tau / \partial T^{-1})_p$$

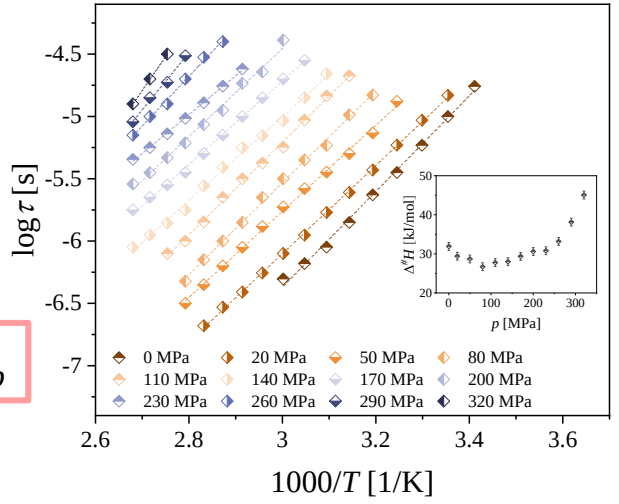

A. Drzewicz, M. Jasiurkowska-Delaporte, E. Juszyńska-Gałązka, W. Zając, P. Kula, *Effect of high pressure on relaxation dynamics and crystallization kinetics of liquid crystal*, prepared

Pressure-induced melt crystallization (mc) kinetics of 3F7HPhH7

Avrami plots under various (T, p) conditions for pressure-induced mc (**BDS**). Inset presents temperature dependence of the characteristic time of mc.

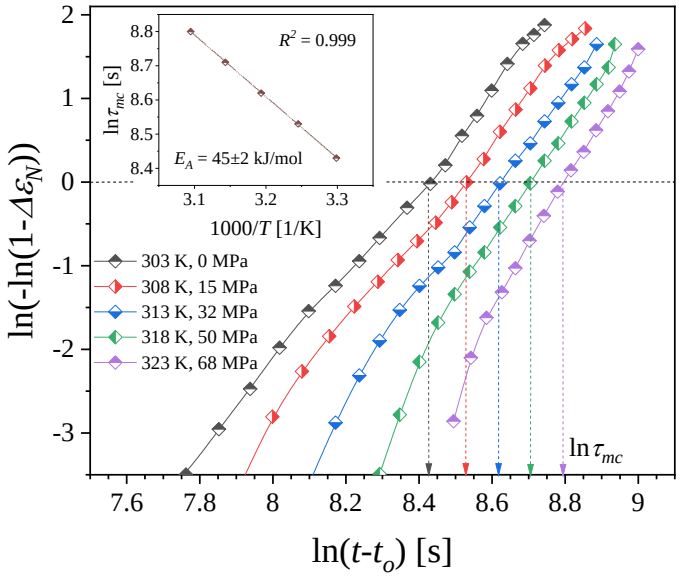

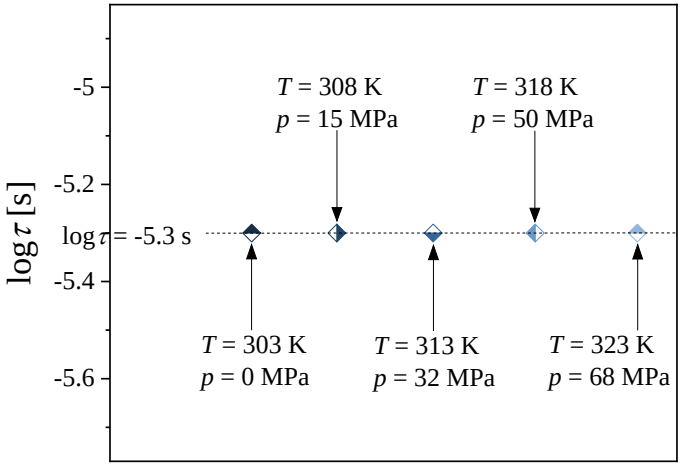

$$n_A \sim 4$$

$$\nearrow \tau_{mc} \text{ and } \searrow \ln K \text{ with } \nearrow (T, p)$$

kinetics of pressure-induced mc of 3F7HPhH7 depends primarily on **nucleation**

Avrami model:

$$\Delta\varepsilon_N(t) = 1 - \exp(-K(t - t_o)^{n_A})$$

Logarithmic form:

$$\log(-\ln(1 - \Delta\varepsilon_N(t))) = \log K + n_A \log(t - t_o)$$

A. Drzewicz, M. Jasiurkowska-Delaporte, E. Juszyńska-Gałązka, W. Zając, P. Kula, *Effect of high pressure on relaxation dynamics and crystallization kinetics of liquid crystal*, prepared M. Avrami, *J. Chem. Phys.*, **1939**, 7, 1103; M. Avrami, *J. Chem. Phys.*, **1940**, 8, 212

What happens during Fast Cooling and next Heating?

Fast cooling and next heating of 3F7HPhH7

DSC thermograms

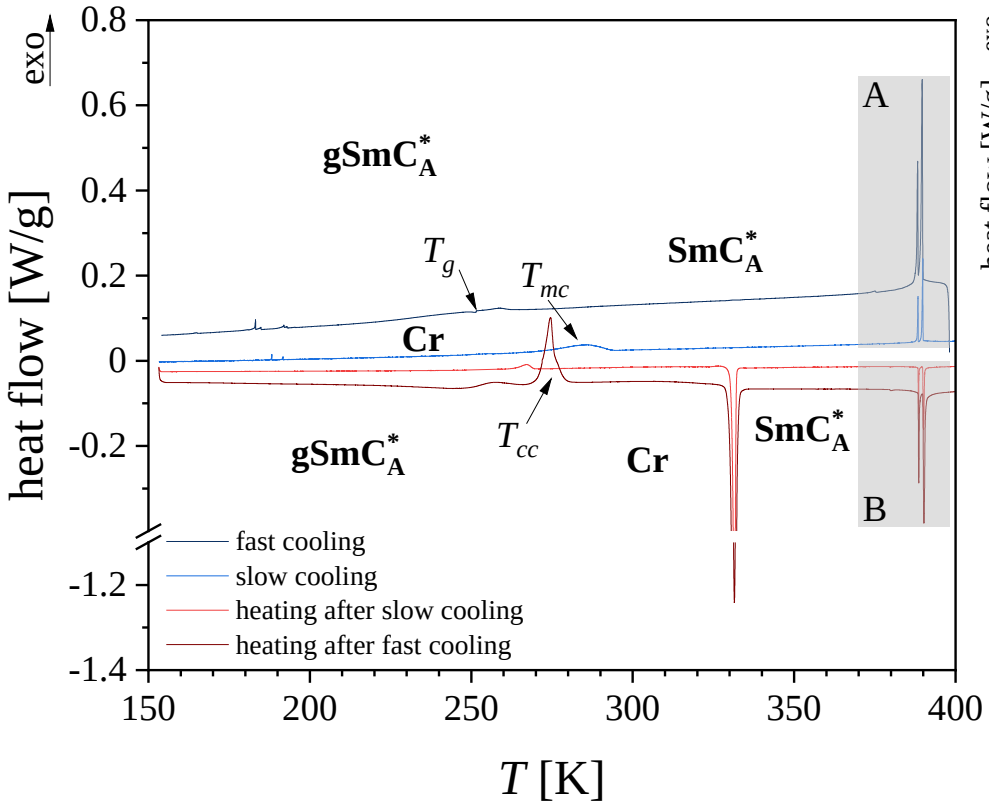

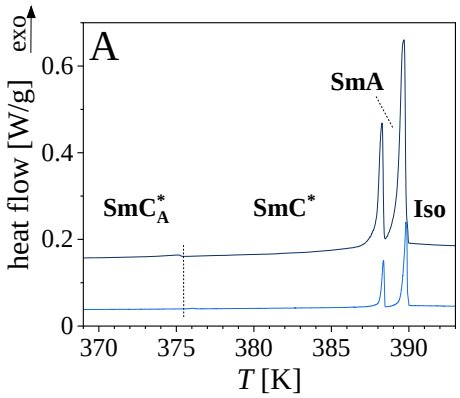

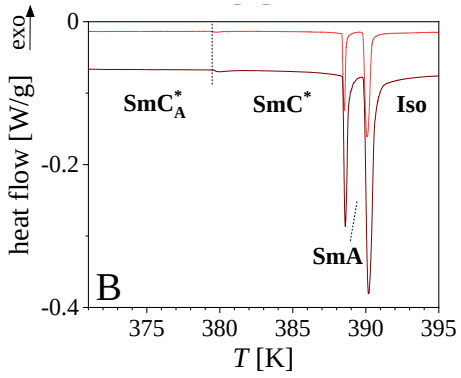

DSC and **BDS** (heating)

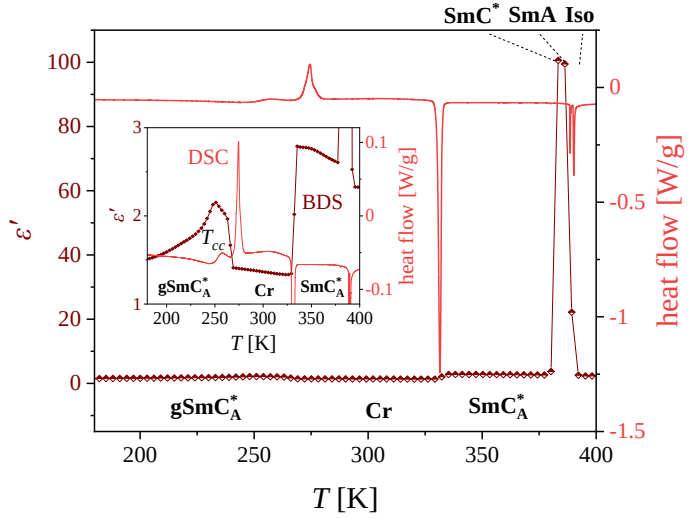

A. Drzewicz, M. Jasiurkowska-Delaporte, E. Juszyńska-Gałązka, M. Piwowarczyk, W. Zając, P. Kula, *On relaxation dynamics of double glass-forming antiferroelectric liquid crystal*, prepared

Relaxation dynamics of 3F7HPhH7 during heating after fast cooling

Activation plots during heating after fast cooling

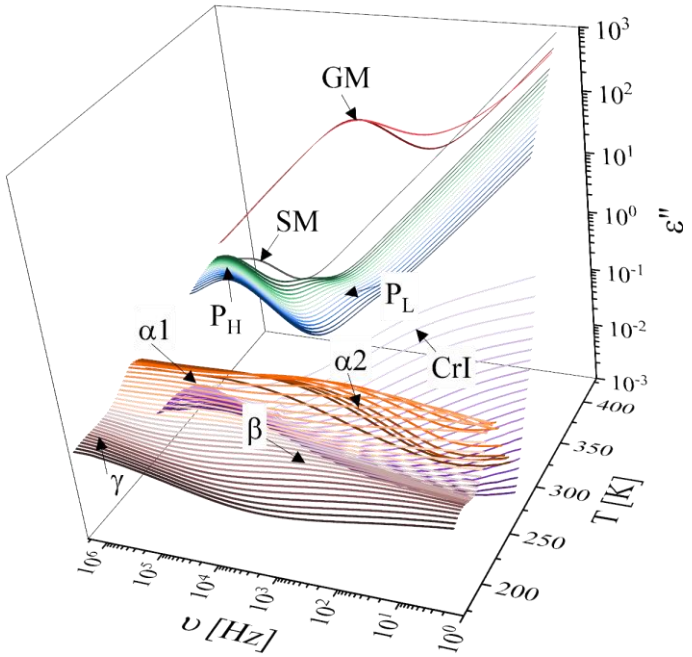

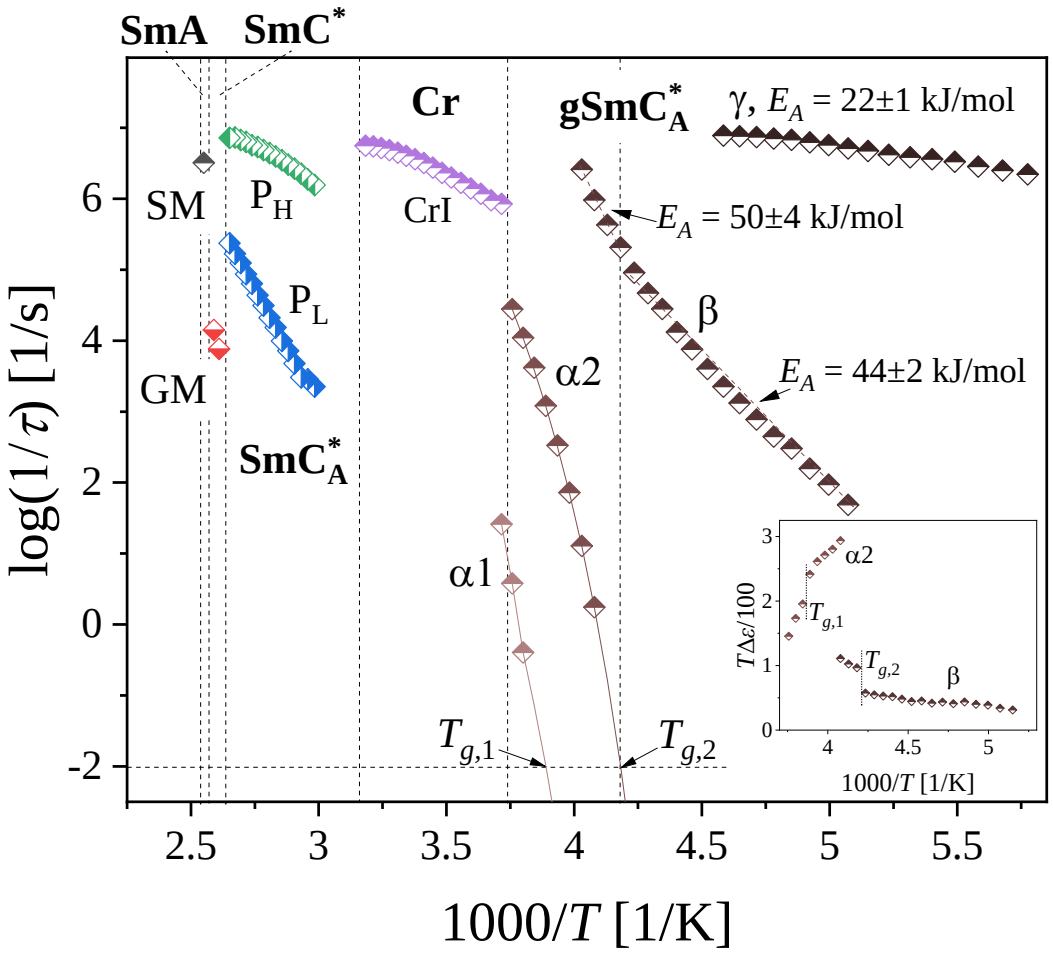

Vogel-Fulcher-Tammann equation (VFT):

$$\tau_\alpha = \tau_\infty \exp\left(\frac{D_f T_0}{T - T_0}\right)$$

where:

τ_α - structural α-relaxation time, τ_∞ - pre-exponential factor,

D_f - constant parameter, T_0 - Vogel temperature.

A. Drzewicz, M. Jasiurkowska-Delaporte, E. Juszyńska-Gałązka, M. Piwowarczyk, W. Zając, P. Kula, *On relaxation dynamics of double glass-forming antiferroelectric liquid crystal*, prepared M.D. Ediger, C.A. Angell, S.R. Nagel, *J. Phys. Chem.*, **1996**, 100, 13200

Relaxation dynamics of 3F7HPhH7 during heating after fast cooling

Activation plots during heating after fast cooling

Fragility index m_f:

$$m_f = \left.\frac{d \log \tau_\alpha}{d(T_g/T)}\right|_{T=T_g}$$

$m_f \sim 16$ – strong glasses,
m_f up to 200 – fragile glasses.

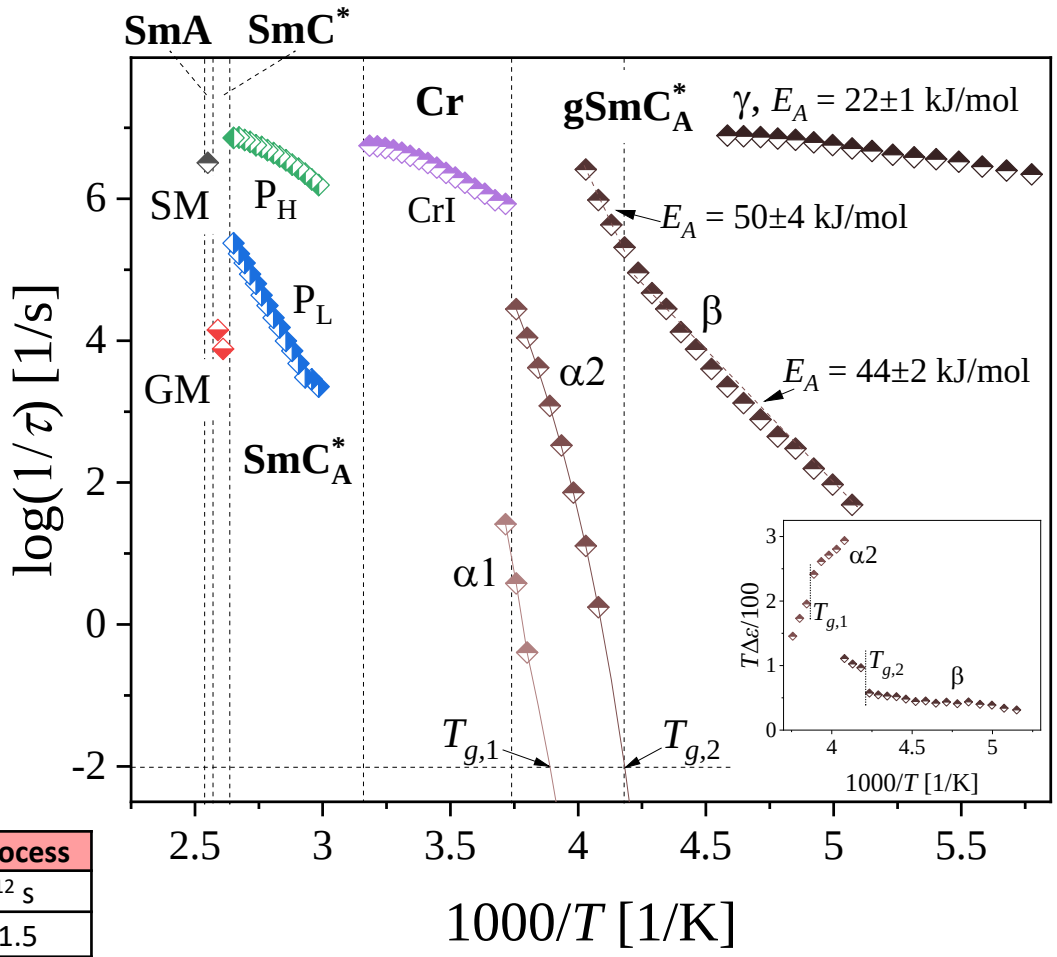

VFT parameters ofα1–process		VFT parameters ofα2–process	
τ_∞	$1 \cdot 10^{-12}$ s	τ_∞	$1 \cdot 10^{-12}$ s
D_f	4.4 ± 1.1	D_f	4.9 ± 1.5
T_0	228 ± 2 K	T_0	207 ± 3 K
$T_{g,1}$	259 ± 4 K	$T_{g,2}$	239 ± 5 K
m_f	150 ± 5	m_f	136 ± 6

A. Drzewicz, M. Jasiurkowska-Delaporte, E. Juszyńska-Gałązka, M. Piwowarczyk, W. Zając, P. Kula, *On relaxation dynamics of double glass-forming antiferroelectric liquid crystal*, prepared
C.A. Angell, *Science*, **1995**, 267, 1924

Vibrational dynamics of 3F7HPhH7 during heating after fast cooling

$\Delta\nu = \nu_T - \nu_{259\,K}$

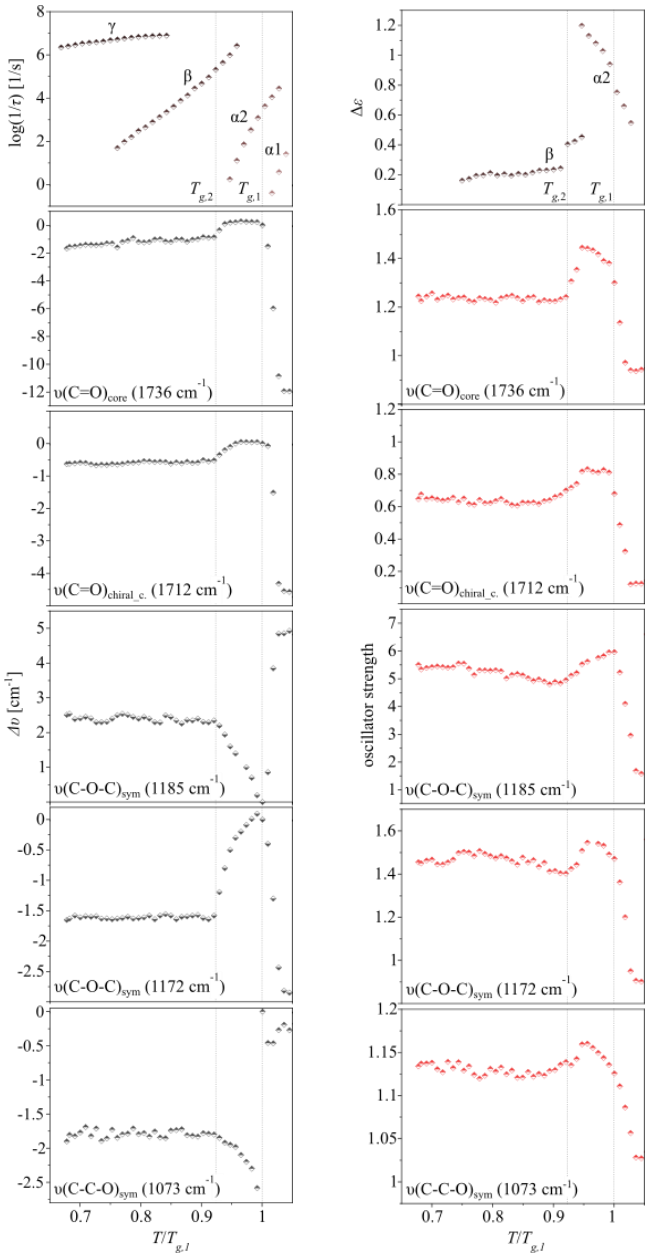

Comparison of dynamics (from **BDS**) and **IR** vibrational properties as a function of $T/T_{g,1}$

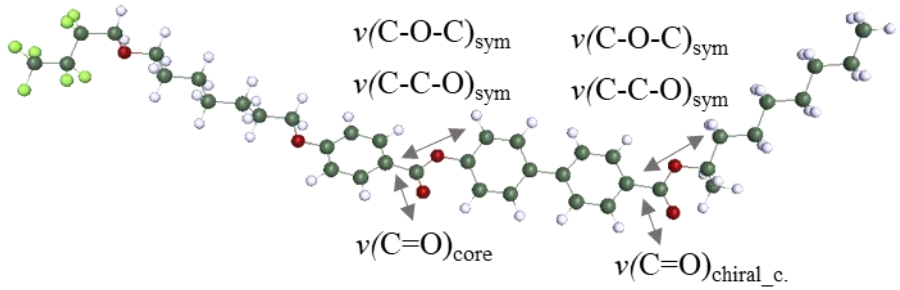

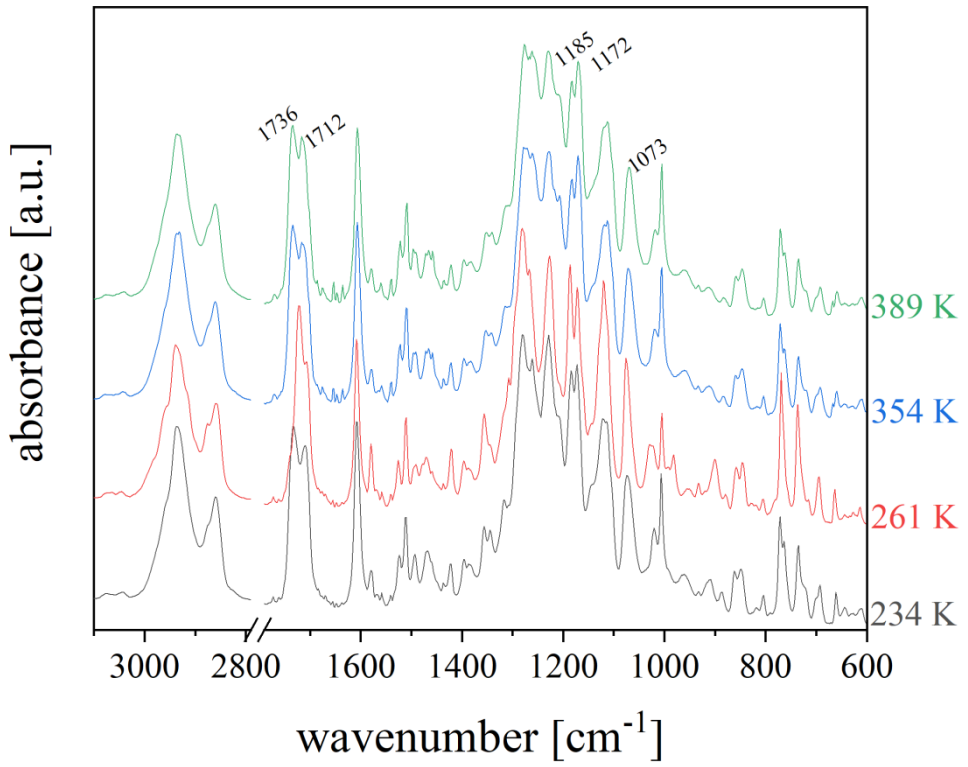

A. Drzewicz, M. Jasiurkowska-Delaporte, E. Juszyńska-Gałązka, M. Piwowarczyk, W. Zając, P. Kula, *On relaxation dynamics of double glass-forming antiferroelectric liquid crystal*, prepared

A. Drzewicz, E. Juszyńska-Gałązka, W. Zając, P. Kula, *Crystals*, **2020**, 10, 1

Isothermal and Non-isothermal Cold Crystallization

Crystallization vs. cold crystallization

Two steps of crystallization:

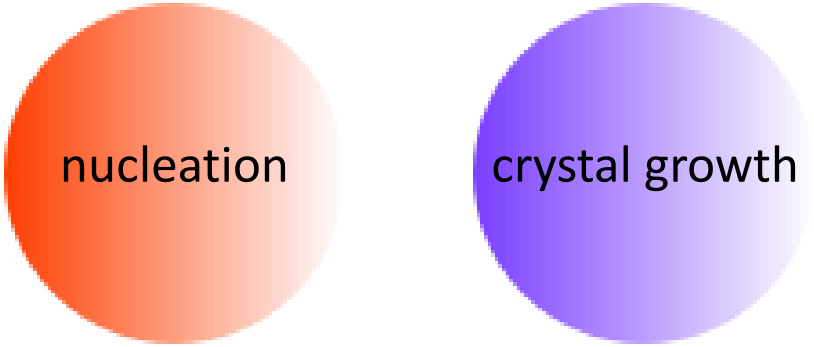

Crystallization during cooling:

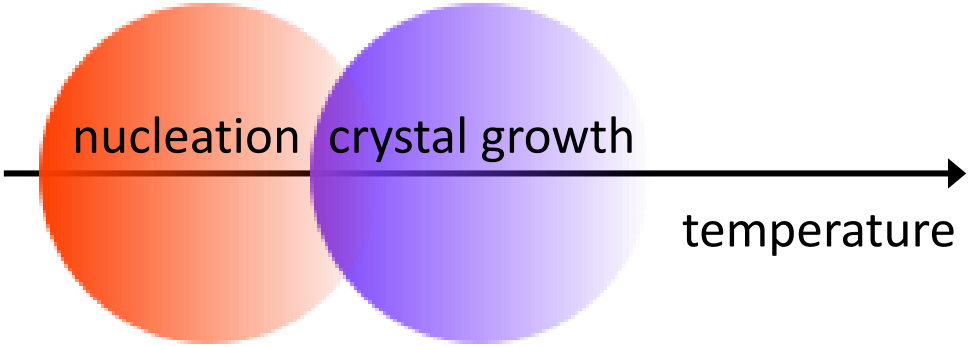

Cold crystallization during heating:

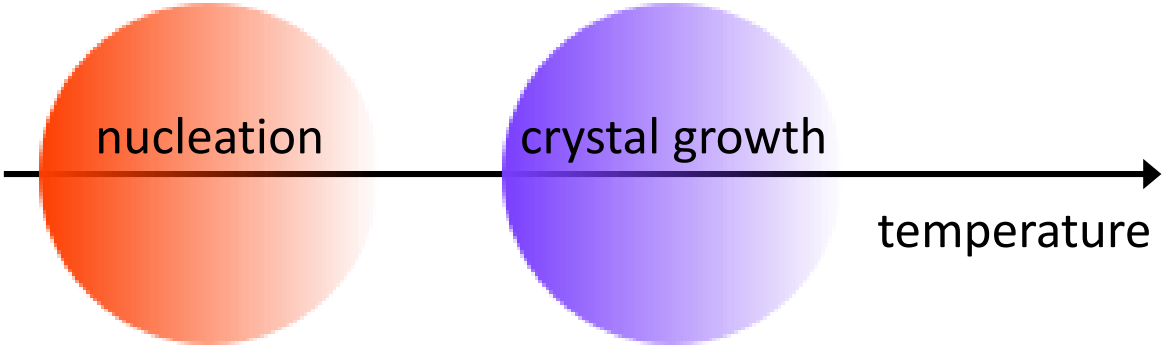

or cooling fast enough to avoid crystallization

Isothermal cold crystallization (cc) of 3F7HPhH7

Avrami plots at T_{cc} for isothermal cc (**DSC**).
The inset presents temperature dependence of the characteristic time of cc.

$n_A \sim 3$
↘ τ_{cr} **and** ↗ $\ln k$ **with** ↗ T

↓

kinetics of isothermal cc of 3F7HPhH7 depends primarily on **diffusion rates**

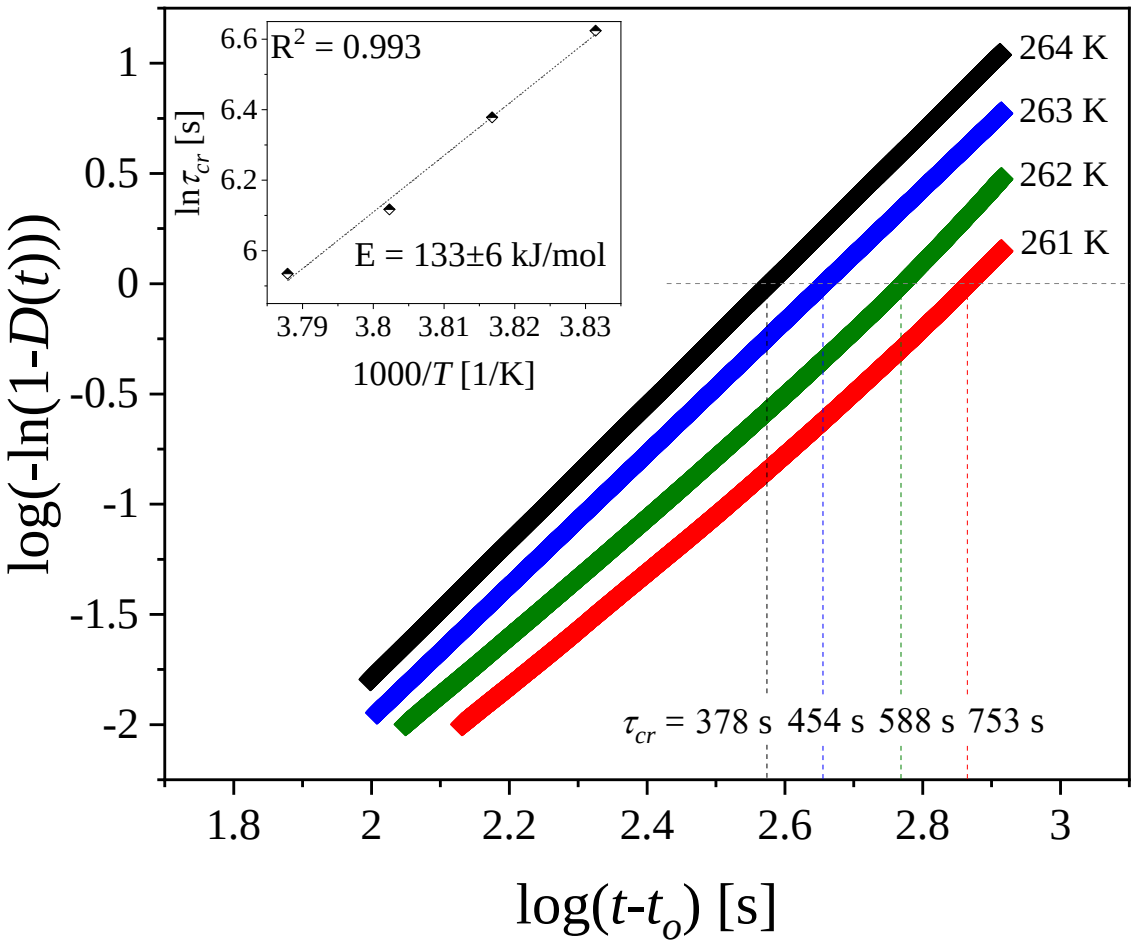

Avrami model:

$$D(t) = 1 - \exp(-k(t - t_o)^{n_A})$$

Logarithmic form:

$$\log(-\ln(1 - D(t))) = \log k + n_A \log(t - t_o)$$

where:
k – depends on nucleation and crystal growth,
t_o - the induction time of crystallization,
n_A - Avrami exponent.

A. Drzewicz, E. Juszyńska-Gałązka, W. Zając, M. Piwowarczyk, W. Drzewiński, *J. Mol. Liq.*, **2020**, 319, 114153
M. Avrami, *J. Chem. Phys.*, **1939**, 7, 1103; M. Avrami, *J. Chem. Phys.*, **1940**, 8, 212

Isothermal cold crystallization (cc) of 3F7HPhH7

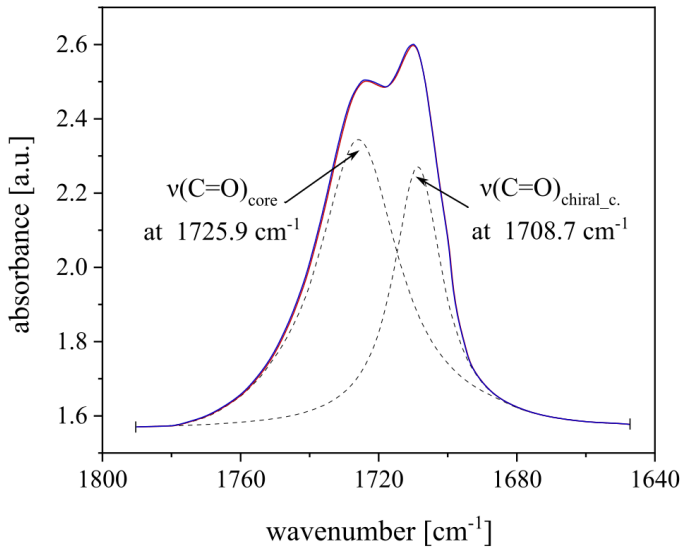

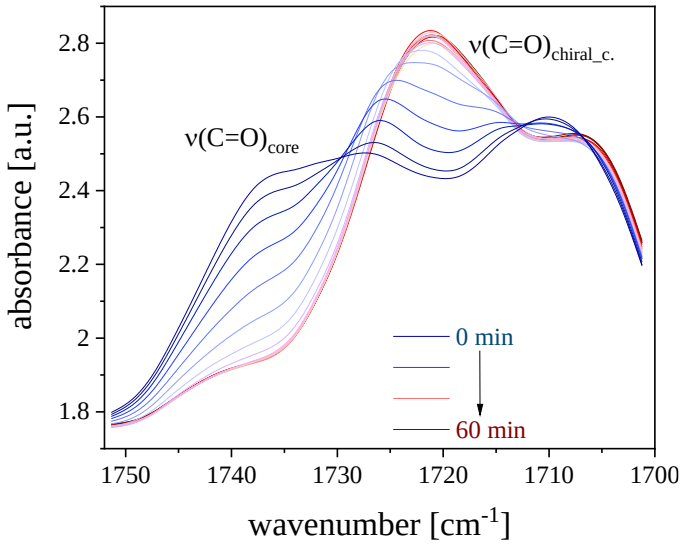

Avrami plots for isothermal cc at 261 K (**FTIR**).

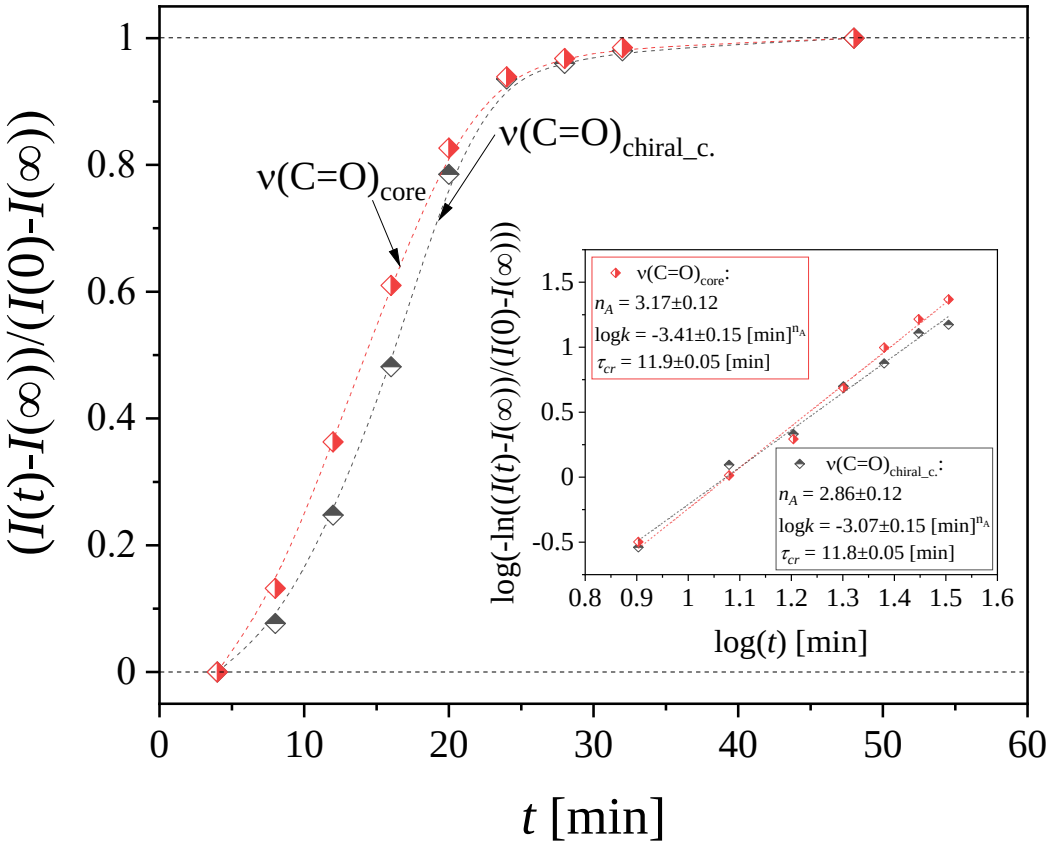

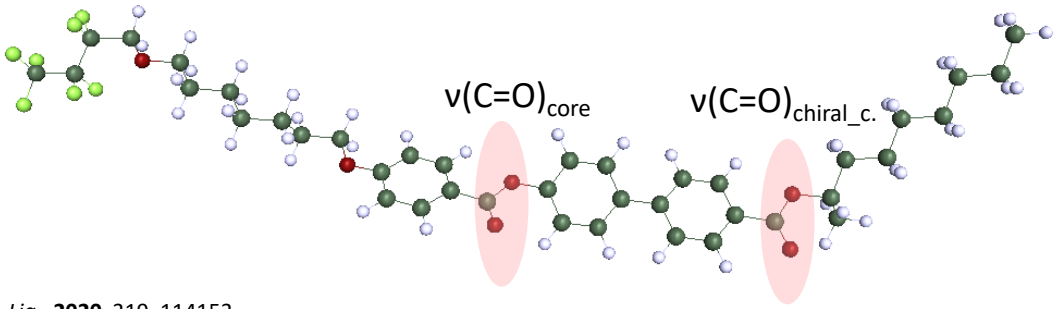

A. Drzewicz, E. Juszyńska-Gałązka, W. Zając, M. Piwowarczyk, W. Drzewiński, *J. Mol. Liq.*, **2020**, 319, 114153

Isothermal cold crystallization (cc) of 3F7HPhH7

Time evolution of **BDS** parameters during isothermal cc at 261 K:

dielectric permittivity ε'

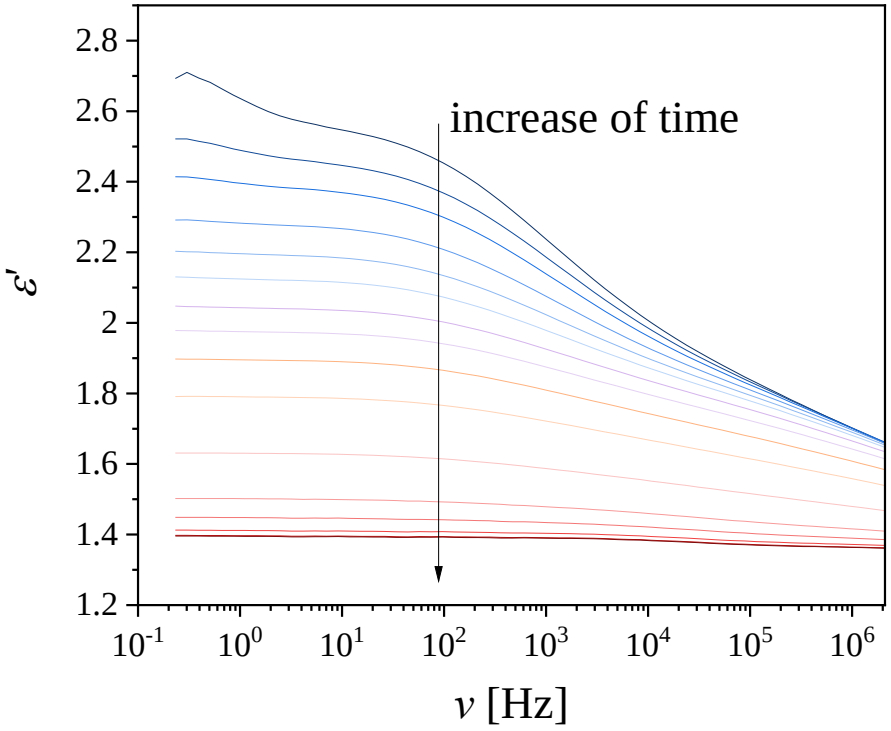

dielectric loss ε'' spectra

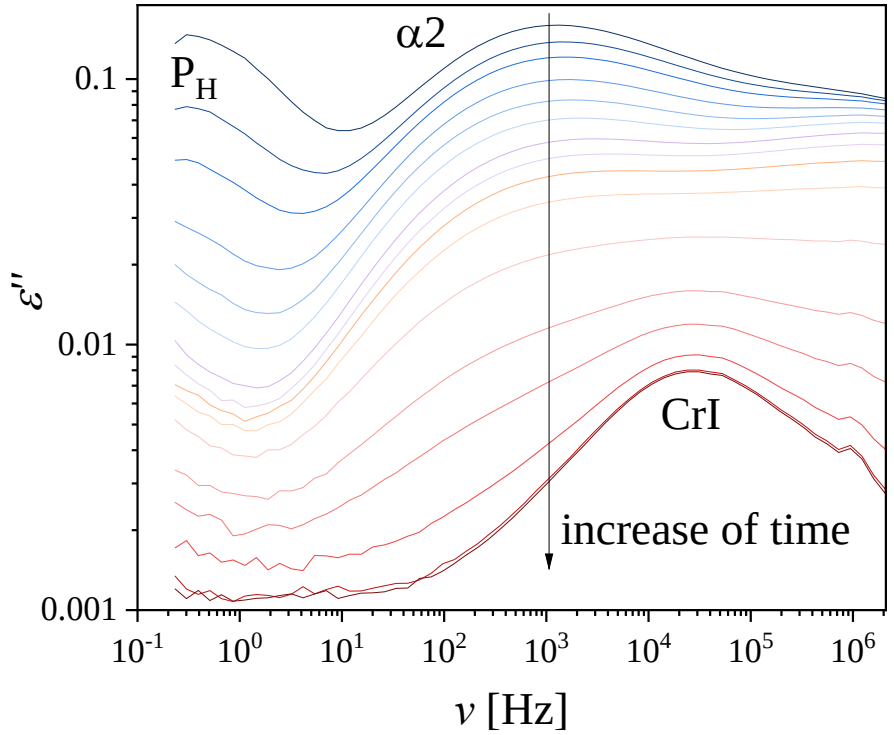

A. Drzewicz, M. Jasiurkowska-Delaporte, E. Juszyńska-Gałązka, M. Piwowarczyk, W. Zając, P. Kula, *On relaxation dynamics of double glass-forming antiferroelectric liquid crystal*, prepared

Non-isothermal cold crystallization (cc) of 3F7HPhH7

Ozawa plots for non-isothermal cc (**DSC**).

$n_O \sim 3$

slow heating: ↗ $\log Z$ **with** ↗ T

↓

depends on **diffusion rates**

fast heating: ↘ $\log Z$ **with** ↗ T

↓

depends on **nucleation**

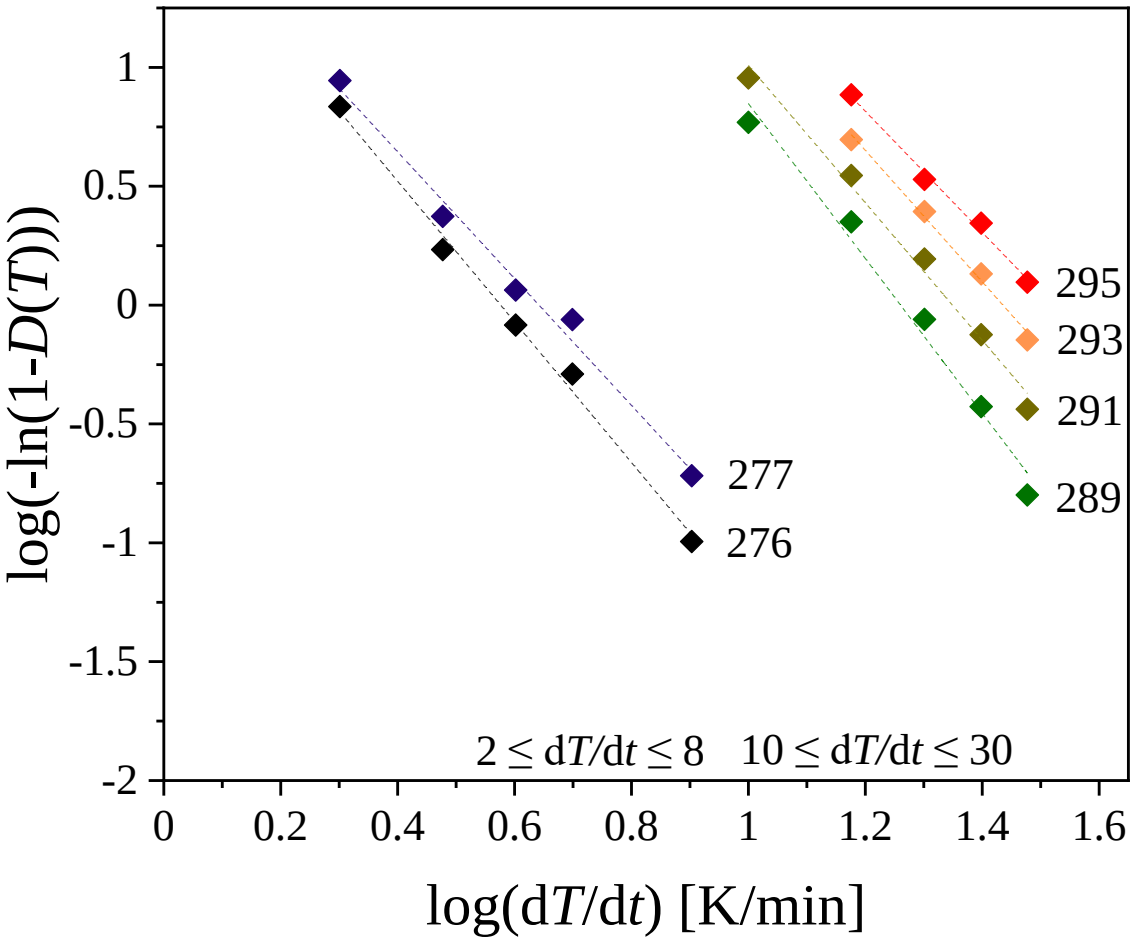

Ozawa model:

$$D(T) = 1 - \exp\left(-\frac{Z}{(\mathrm{d}T/\mathrm{d}t)^{n_O}}\right)$$

Logarithmic form:

$$\log\left(-\ln(1 - D(T))\right) = \log Z - n_O \log(\mathrm{d}T/\mathrm{d}t)$$

where:
Z – the Ozawa crystallization rate,
n_O - Ozawa exponent.

A. Drzewicz, E. Juszyńska-Gałązka, W. Zając, M. Piwowarczyk, W. Drzewiński, *J. Mol. Liq.*, **2020**, 319, 114153
T. Ozawa, *Polymer*, **1971**, 12, 150

Non-isothermal cold crystallization (cc) of 3F7HPhH7

Mo plots for non-isothermal cc (**DSC**).

Two different mechanisms of non-isothermal cc, depending on the range of heating rates

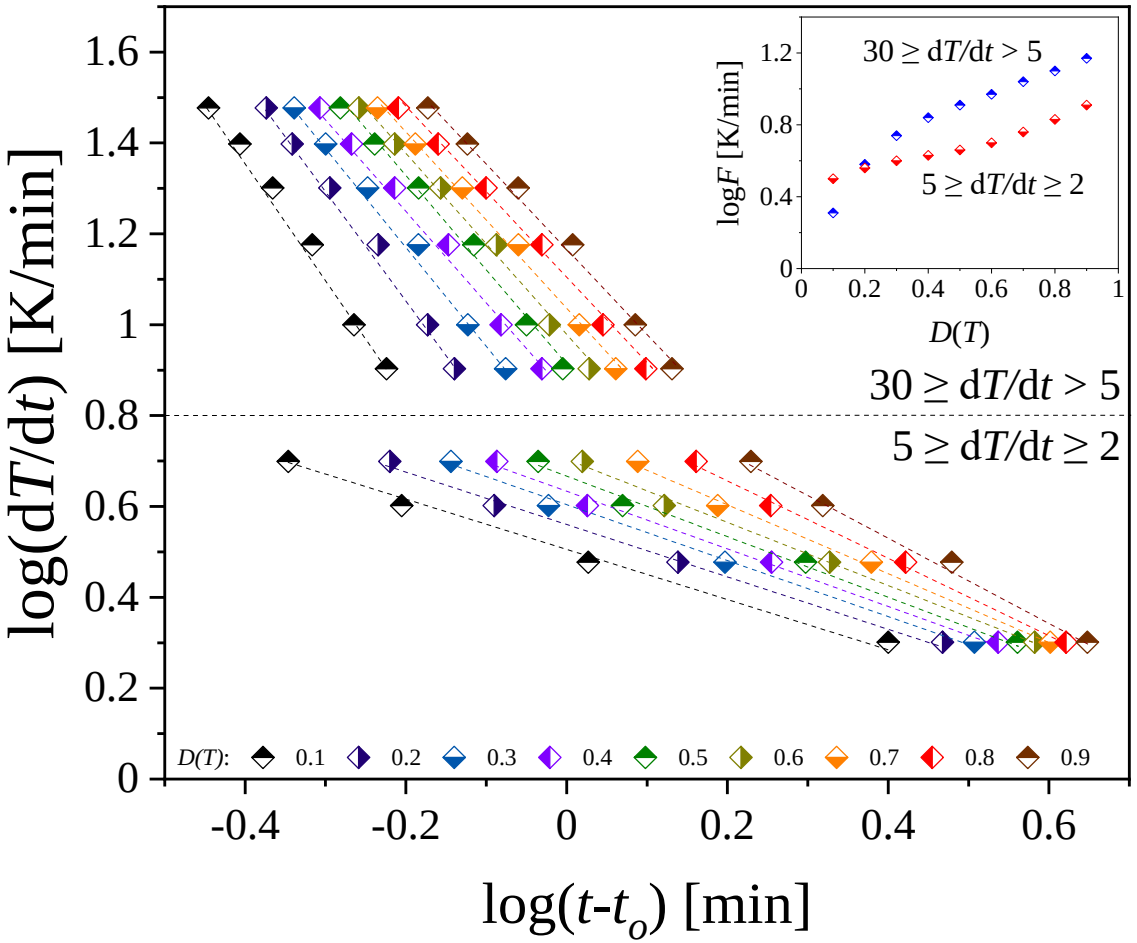

Mo model:

$$\log k + n_A \log(t - t_o) = \log Z - n_O \log\left(\frac{\mathrm{d}T}{\mathrm{d}t}\right)$$

$$\log(\mathrm{d}T/\mathrm{d}t) = \log F - a \cdot \log(t - t_o)$$

where:
F – related to the cooling/heating rate,
a - the ratio of Avrami n_A exponent to Ozawa n_O exponent.

A. Drzewicz, E. Juszyńska-Gałązka, W. Zając, M. Piwowarczyk, W. Drzewiński, *J. Mol. Liq.*, **2020**, 319, 114153
T. Liu, Z. Mo, S. Wang, H. Zhang, *Polym. Eng. Sci.*, **1997**, 37, 568

Non-isothermal cold crystallization (cc) of 3F7HPhH7

Kissinger and Augis-Benett plots for non-isothermal cc (**DSC**).

Two distinct regions of different linear dependences, corresponding to heating rates

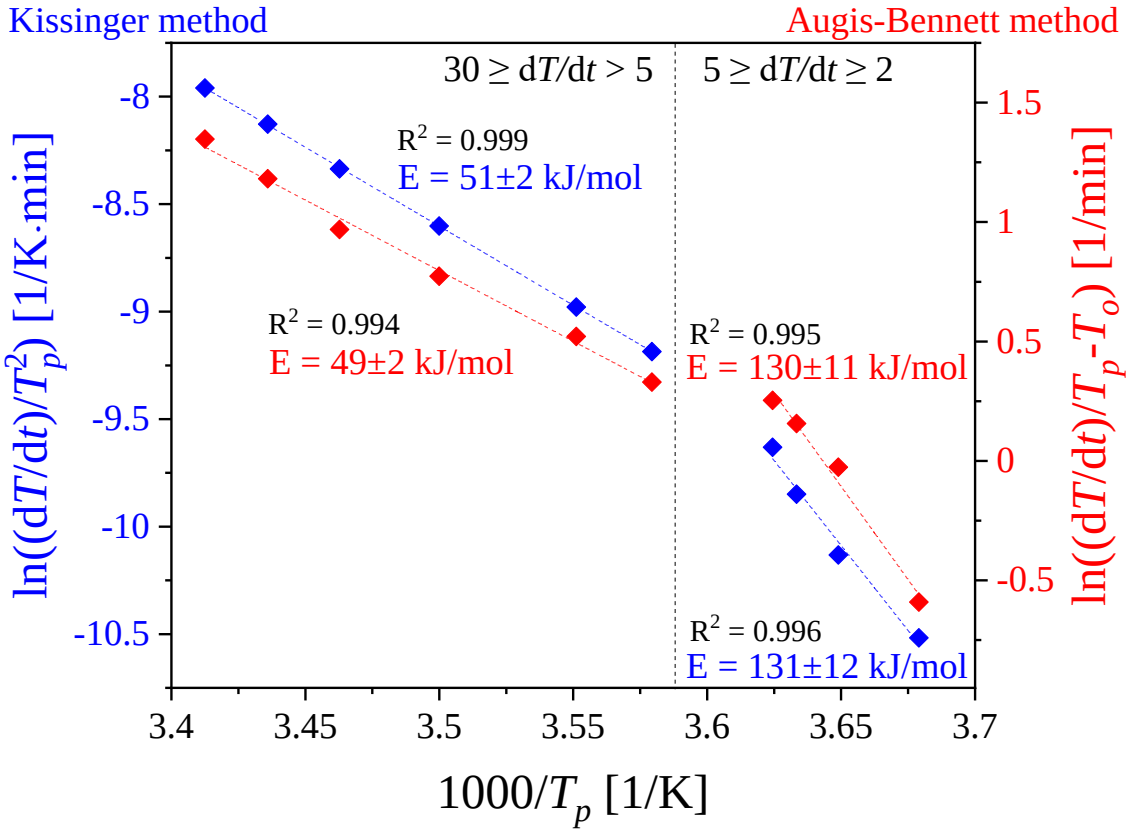

Kissinger model:

$$\ln\left(\frac{\mathrm{d}T/\mathrm{d}t}{T_p^2}\right) = -\frac{E}{RT_p} + const$$

Augis-Bennett model:

$$\ln\left(\frac{\mathrm{d}T/\mathrm{d}t}{T_p - T_o}\right) = -\frac{E}{RT_p} + const$$

where:
T_p - the maximum of the crystallization peak,
T_o - the initial crystallization temperature,
R – the gas constant,
E – the activation energy.

A. Drzewicz, E. Juszyńska-Gałązka, W. Zając, M. Piwowarczyk, W. Drzewiński, *J. Mol. Liq.*, **2020**, 319, 114153
H.E. Kissinger, *J. Res. Natl. Inst. Stand. Technol.*, **1956**, 57, 217; J.A. Augis, J.E. Bennett, *J. Therm. Anal. Calorim.*, **1978**, 13, 283

Conclusions

Slow cooling of 3F7HPhH7 causes its crystallization, while fast cooling results in its vitrification.

BDS spectra show the weak CrI mode in the Cr phase of 3F7HPhH7, so it suggests that the observed Cr phase is conformationally disordered (CONDIS) crystal type.

Pressure-induced melt crystallization of 3F7HPhH7 studied under isochronal conditions depends primarily on the formation of nuclei.

Two glass transitions of 3F7HPhH7 were found at $T_{g,1} = 239\ \mathrm{K}$ and $T_{g,2} = 259\ \mathrm{K}$ which are associated with freezing of anti-phase motions and reorientation around long molecular axis in the SmC_A^* phase, respectively.

Non-isothermal cold crystallization in 3F7HPhH7 occurs via diffusion when the sample is heated slowly (as under isothermal conditions), while during fast heating, nucleation phenomena dominate the process.

ACKNOWLEDGEMENT

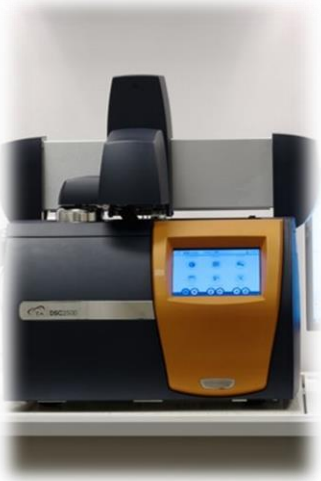

Financial support of the Director of IFJ PAN

ACKNOWLEDGEMENT

Wojciech ZAJĄC, Assoc. Prof.

Ewa JUSZYŃSKA-GAŁĄZKA, Assoc. Prof.

Małgorzata JASIURKOWSKA-DELAPORTE, Ph. D.

Aleksandra DEPTUCH, Ph. D.

Marcin PIWOWARCZYK, M. Sc., Ph. D. student

Przemysław KULA, Assoc. Prof.

THANK YOU FOR YOUR ATTENTION ☺